

## Atmospheric chemistry results from the ANTCI 2005 Antarctic plateau airborne study

D. L. Slusher,<sup>1</sup> W. D. Neff,<sup>2</sup> S. Kim,<sup>3</sup> L. G. Huey,<sup>3</sup> Y. Wang,<sup>3</sup> T. Zeng,<sup>3</sup> D. J. Tanner,<sup>3</sup> D. R. Blake,<sup>4</sup> A. Beyersdorf,<sup>4</sup> B. L. Lefer,<sup>5</sup> J. H. Crawford,<sup>6</sup> F. L. Eisele,<sup>7</sup> R. L. Mauldin,<sup>7</sup> E. Kosciuch,<sup>7</sup> M. P. Buhr,<sup>8</sup> H. W. Wallace,<sup>8</sup> and D. D. Davis<sup>3</sup>

Received 10 June 2009; revised 19 October 2009; accepted 20 November 2009; published 13 April 2010.

[1] One of the major goals of the 2005 Antarctic Tropospheric Chemistry Investigation (ANTCI) was to bridge the information gap between current knowledge of South Pole (SP) chemistry and that of the plateau. The former has been extensively studied, but its geographical position on the edge of the plateau makes extrapolating these findings across the plateau problematic. The airborne observations reported here demonstrate that, as at SP, elevated levels of nitric oxide (NO) are a common summertime feature of the plateau. As in earlier studies, planetary boundary layer (PBL) variations were a contributing factor leading to NO fluctuations. Thus, extensive use was made of in situ measurements and models to characterize PBL depths along each flight path and over broader areas of the plateau. Consistent with earlier SP studies that revealed photolysis of nitrate in surface snow as the source of NO<sub>x</sub>, large vertical gradients in NO were observed over most plateau areas sampled. Similar gradients were also found for the nitrogen species HNO<sub>3</sub> and HO<sub>2</sub>NO<sub>2</sub> and for O<sub>3</sub>. Thus, a common meteorological-chemical feature found was shallow PBLs associated with nitrogen species concentrations that exceeded free tropospheric levels. Collectively, these new results greatly extend the geographical sampling footprint defined by earlier SP studies. In particular, they suggest that previous assessments of the plateau as simply a chemical depository need updating. Although the evidence supporting this position comes in many forms, the fact that net photochemical production of ozone occurs during summer months over extensive areas of the plateau is pivotal.

**Citation:** Slusher, D. L., et al. (2010), Atmospheric chemistry results from the ANTCI 2005 Antarctic plateau airborne study, *J. Geophys. Res.*, 115, D07304, doi:10.1029/2009JD012605.

### 1. Introduction

[2] There has been growing evidence over the last decade that polar regions can display very diverse chemistry during the summer months. This is particularly true as it relates to the chemistry occurring in surface snow [e.g., *Domine and Shepson*, 2002; *Grannas et al.*, 2007, and references therein]. Furthermore, it is now apparent that this snow chemistry can play a major role in ultimately defining the chemistry of the overlying atmosphere in polar regions. Levels of envi-

ronmentally important species such as ozone and mercury are frequently found to be linked to this newly recognized chemistry. Additionally, studies have revealed that the near-surface atmosphere at some of the most remote polar sites in the world (e.g., South Pole (SP), Antarctica) undergo extraordinary shifts in the levels of critical oxidizing species such as the hydroxyl radical (OH) [*Davis et al.*, 2008; *Mauldin et al.*, 2001, 2004; *Wang et al.*, 2008].

[3] These new findings also appear to be of considerable significance in understanding the planet's climate history. For example, one of the richest sources of global climate information is the polar ice of Antarctica [*Legrand and Delmas*, 1987; *Legrand and Feniet-Saigne*, 1991]. Since this information is mostly contained in the form of chemical proxy species, interpretation typically requires a detailed understanding of the sources, sinks, and transport of these same species in today's atmosphere. Efforts to date to interpret the proxy chemical family labeled reactive nitrogen have resulted in minimal success [*Legrand and Kirchner*, 1990; *Legrand and Mayewski*, 1997; *Wolff et al.*, 1995, 2008]. Reactive nitrogen could potentially provide insight into the oxidizing capacity of the planet's past atmosphere. For example, as in today's atmosphere, reactive nitrogen is

<sup>1</sup>Department of Chemistry and Physics, Coastal Carolina University, Conway, South Carolina, USA.

<sup>2</sup>Earth System Research Laboratory, NOAA, Boulder, Colorado, USA.

<sup>3</sup>School of Earth and Atmospheric Sciences, Georgia Institute of Technology, Atlanta, Georgia, USA.

<sup>4</sup>School of Physical Sciences, University of California, Irvine, California, USA.

<sup>5</sup>Department of Earth and Atmospheric Sciences, University of Houston, Houston, Texas, USA.

<sup>6</sup>NASA Langley Research Center, Hampton, Virginia, USA.

<sup>7</sup>National Center for Atmospheric Research, Boulder, Colorado, USA.

<sup>8</sup>Air Quality Design, Golden, Colorado, USA.

believed to have played a major role in prehistoric times in maintaining the levels of both OH and O<sub>3</sub>, two of the most important atmospheric oxidizing agents [Finlayson-Pitts and Pitts, 2000, and references therein].

[4] Although emissions of reactive nitrogen in the form of NO<sub>x</sub> (NO + NO<sub>2</sub>) have been reported at several polar sites [Beine *et al.*, 2002a, 2002b; Davis *et al.*, 2001, 2004, 2008; Honrath *et al.*, 1999, 2000a, 2000b; Jones *et al.*, 2000; Ridley *et al.*, 2000], nowhere has it resulted in such large-scale atmospheric perturbations as seen at SP, Antarctica [Chen *et al.*, 2001, 2004; Crawford *et al.*, 2001; Davis *et al.*, 2001, 2004, 2008; Helmig *et al.*, 2008a, 2008b; Mauldin *et al.*, 2001, 2004; Wang *et al.*, 2008]. Representative of these perturbations, during the Investigation of Sulfur Chemistry in the Antarctic Troposphere (ISCAT) studies in 1998 and 2000, NO concentrations ranging from 10 to 600 pptv were observed. As a result, net photochemical production of ozone was a common chemical occurrence in the near-surface atmosphere [Crawford *et al.*, 2001; Helmig *et al.*, 2008a; Johnson *et al.*, 2008; Oltmans *et al.*, 2008]. Highly elevated OH levels were also measured throughout the austral late spring/summer period [Mauldin *et al.*, 2001, 2004, 2009]. Similar to the findings at other polar sites [Honrath *et al.*, 1999, 2000a, 2000b; Jones *et al.*, 2000], SP studies have shown that photodenitrification of surface snow containing nitrate is the dominant source of NO<sub>x</sub>. Making the argument that this same phenomenon is common to the more expansive plateau region, however, has been difficult to justify. One of the compelling counterarguments has been that SP defines an extremely small area in comparison to the plateau, a region approximately the size of the continental United States. In addition, SP is geographically situated near the western edge of the plateau and lacks a diurnal solar heating cycle. Farther north, greatly enhanced daytime mixing could prevent the accumulation of NO<sub>x</sub> in shallow boundary layers.

[5] During the 2003 Antarctic Tropospheric Chemical Investigation (ANTCI), aircraft observations of NO and NO<sub>y</sub> extended the SP sampling footprint out to distances of ~400 km [Davis *et al.*, 2008]. Although representing a significant step forward, these limited measurements still left many questions about the areal extent of this new chemistry unanswered. This paper focuses on the Antarctic airborne observations recorded during the austral spring/summer of 2005 (ANTCI 2005). The primary objective of this program was to greatly extend substantially the areal observations of NO and chemically related species, using the Twin Otter aircraft as a sampling platform. More specifically, it was designed to reach geographical regions of the plateau far removed from SP, especially those at higher elevations and at significantly different latitudes. A critical component of this objective was to compare these new observations with those recorded at SP to determine the degree of chemical commonality between these different sites. Given that SP studies have shown that the planetary boundary layer (PBL) depth can play a significant role in dictating NO<sub>x</sub> levels, a major effort was also made in this study to characterize the meteorological environment along all aircraft flight paths. This involved using a combination of aircraft-generated temperature profiles, satellite data, modeling products, and remote-site surface observations on the plateau. A secondary objective was to explore further the

chemical relationships between NO<sub>x</sub> and other labile species measured, including O<sub>3</sub>, HNO<sub>3</sub>, HO<sub>2</sub>NO<sub>2</sub>, SO<sub>2</sub>, and H<sub>2</sub>SO<sub>4</sub>.

## 2. Sampling Platform, Measurement Techniques, and Modeling

[6] The DHC-6 Twin Otter aircraft used in the ANTCI 2005 field study had a working radar altitude range (i.e., altitude above snow surface) of 15–1000 m while operating on the plateau. Approximately 50% of the plateau data were collected below 150 m, 74% were collected below 500 m, and 95% were collected below 1000 m. This vertical sampling range is similar to that in ANTCI 2003 [Davis *et al.*, 2008]; however, a larger fraction of the flights were below 500 m in the 2003 study. The horizontal range of the aircraft during ANTCI 2005 was greatly extended over that in 2003, primarily by establishing refueling sites between the point of departure and the final destination. For example, two refueling stops were required during flight 5 (i.e., McMurdo to SP). During flight 7, there were three refuelings. Details regarding each of the individual flights are reported in Table 2 and in section 3.

[7] Chemical species measured during this study and the techniques employed for their measurement are listed in Table 1. For the species NO, O<sub>3</sub>, HNO<sub>3</sub>, HO<sub>2</sub>NO<sub>2</sub>, SO<sub>2</sub>, methanesulfonic acid, and H<sub>2</sub>SO<sub>4</sub>, measurements were submitted to the data archive with 1 min resolution. Grab samples of several other species were collected via stainless steel canisters and later analyzed. The number of grab samples collected per flight varied but typically ranged from 15 to 30. Species measured in this mode included dimethyl sulfide (DMS), carbonyl sulfide, CO, nonmethane hydrocarbons, and several halocarbons. In addition to the above chemical parameters, the basic aircraft parameters air speed, latitude, longitude, radar altitude, geometric altitude, laser altitude, temperature, and water vapor were recorded. Spectroradiometric data were also recorded for the purpose of evaluating photochemical rate constants during each flight.

## 3. Observations

### 3.1. Overview of ANTCI 2005 Plateau Flight Program

[8] As stated earlier, the primary aim of this paper is to provide a detailed analysis of the airborne field data generated during the ANTCI 2005 study. More specifically, the focus is the data set generated while sampling the plateau. As shown in Figure 1 plateau sampling occurred during all or segments of five flights: 5, 6, 7, 10, and 12. Flights 5–7 were more interior oriented, while flights 10 and 12 tended toward the edges of the plateau, representing areas that might have been influenced by marine inflow. While this set of 5 flights is the main focus of this paper, all 12 ANTCI flights contributed to the development of an overall picture of the plateau's atmospheric chemical environment. For example, flights 4, 9, and 11 provided a contrast of plateau conditions versus those found over coastal environments. Flights 1 and 2 were configured to reveal in greater detail how plateau-generated NO<sub>x</sub> is exported to coastal areas via glacial outflow. Finally, flights 8 and 9 were designed to investigate further the degree to which Mount Erebus volcanic emissions influence trace gas levels on the plateau.

**Table 1.** Measurements Recorded During ANTICI 2005<sup>a</sup>

Compound(s)	Investigator(s)	Technique(s)	Detection Limit
NO	Davis/Buhr/Huey	Chemiluminescence <sup>b</sup>	4 pptv
O <sub>3</sub>	Davis/Buhr	Chemiluminescence <sup>c</sup>	2 ppbv
HNO <sub>3</sub>	Huey	CIMS <sup>d</sup>	5 pptv
HO <sub>2</sub> NO <sub>2</sub>	Huey	CIMS <sup>c</sup>	5 pptv
SO <sub>2</sub>	Huey	CIMS <sup>d</sup>	5 pptv
DMS, OCS, CO	Blake	Grab sample, GC/MS <sup>f</sup>	1 pptv, 10 pptv, 10 ppbv
NMHC and halocarbons	Blake	Grab sample, GC, and GC/MS <sup>f</sup>	0.05–5 pptv <sup>g</sup>
Photochemical <i>J</i> value	Lefer	Spectroradiometer <sup>h</sup>	$\sim 1 \times 10^{-8} \text{ s}^{-1}$
OH, MSA, H <sub>2</sub> SO <sub>4</sub>	Eisele/Mauldin	CIMS	$2 \times 10^5$ to $3 \times 10^5 \text{ mol/cm}^3$ (for 30 s)

<sup>a</sup>Abbreviations are as follows: DMS, dimethyl sulfide; NMHC, nonmethane hydrocarbons; MSA, methanesulfonic acid.

<sup>b</sup>See Ridley and Howlett [1974] and Ridley and Grahek [1990].

<sup>c</sup>See Ridley et al. [1992].

<sup>d</sup>See Huey et al. [2004].

<sup>e</sup>See Slusher et al. [2001].

<sup>f</sup>See Swanson et al. [2004].

<sup>g</sup>Except ethane, which had a detection limit of 20 pptv.

<sup>h</sup>See Lefer et al. [2001] and Shetter and Müller [1999].

[9] In assessing which segments from each flight to use in the final data analysis, latitude, longitude, and elevation were the most critical parameters. Reflecting this filtering scheme, Figure 1 shows the 2000 m elevation contour line used as a guide in defining the dimensions of the plateau. A final filtering exercise was deemed necessary to eliminate individual measurements that might have been contaminated by aircraft engine exhaust. Overall, less than 2% of the recorded database was removed because of this problem.

[10] The time period covered by flights 5–12 was 2–13 December 2005. McMurdo Station was the primary base of operation, though the SP Station also served as the launching point for flights 6 and 7. A brief description of the objectives for flights 5–7, 10, and 12, as well as other ANTICI flights, is given in Table 2. (Note that although flight 3 is also listed in Table 2 as having a plateau sampling objective, most of these data had to be rejected because of instrument problems.) The eight fixed geographical sites

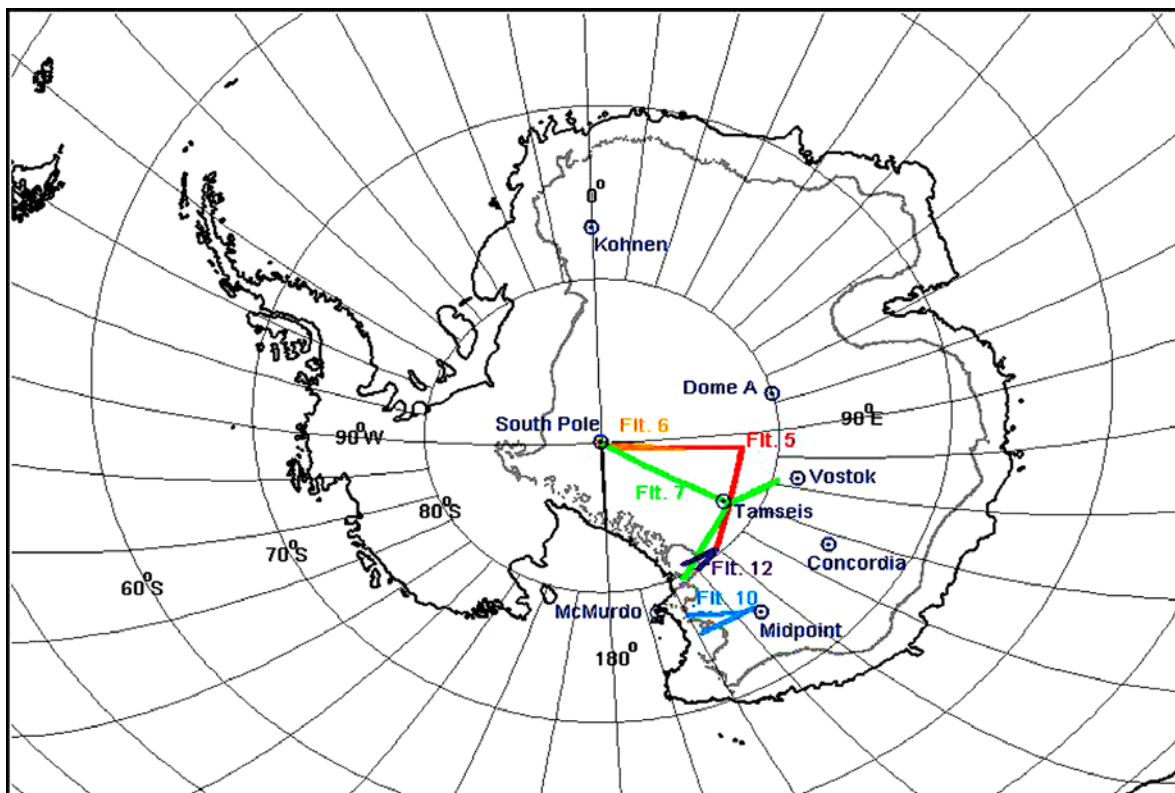


**Figure 1.** Flight track map shows the component of each flight overlapping the Antarctic plateau as defined by the 2000 m contour line. Also shown are the locations of the aircraft landing sites Midpoint (75°S, 145°E) and Tamséis (82°S, 123°E) as well as the geographical sites providing modular equipment transporter (MET) data, which include McMurdo (78°S, 167°E), South Pole (90°S), Vostok (78°S, 107°E), Concordia (75°S, 123°E), Dome A (80°S, 77°E), and Kohlen (77°S, 0°E).

**Table 2.** ANTICI 2005 Flight Dates, Launching Site, and Objectives<sup>a</sup>

Flight Number	Date(s)	Station of Origin	Points Visited/Flight Description	Destination Station
1	20–21 Nov	McMurdo	Reeves Glacier outflow	McMurdo
2	22 Nov	McMurdo	Reeves Glacier outflow	McMurdo
3	24 Nov	McMurdo	Remote sampling via Midpoint (low-Sun condition)	McMurdo
4	30 Nov	McMurdo	Byrd Glacier and Mulock Glacier outflow	McMurdo
<b>5</b>	<b>1–2 Dec</b>	<b>McMurdo</b>	<b>Remote sampling via AGO4 and Tamseis Camp</b>	<b>South Pole</b>
<b>6</b>	<b>3–4 Dec</b>	<b>South Pole</b>	<b>South Pole regional sampling</b>	<b>South Pole</b>
<b>7</b>	<b>4–5 Dec</b>	<b>South Pole</b>	<b>Remote sampling via Vostok Station and Tamseis Camp</b>	<b>McMurdo</b>
8	9 Dec	McMurdo	Mt. Erebus	McMurdo
9	10–11 Dec	McMurdo	Mt. Erebus and sea ice edge	McMurdo
<b>10</b>	<b>11–12 Dec</b>	<b>McMurdo</b>	<b>Remote sampling via Midpoint (high-Sun condition) with return via Reeves Glacier</b>	<b>McMurdo</b>
11	12 Dec	McMurdo	Reeves Glacier inflow and outflow	McMurdo
<b>12</b>	<b>13 Dec</b>	<b>McMurdo</b>	<b>Seismic Center, return via Byrd Glacier</b>	<b>McMurdo</b>

<sup>a</sup>Data on plateau flights are in boldface.

shown in Figure 1 (i.e., McMurdo (78°S, 167°E), Tamseis (82°S, 123°E), SP (90°S), Midpoint (75°S, 145°E), Vostok (78°S, 107°E), Concordia (75°S, 123°E), Dome A (80°S, 77°E), and Kohlen (77°S, 0°E)) represent either designated landing sites for the aircraft or sites providing meteorological data used in sections 3.2 and 4.3.

### 3.2. Meteorological Setting and Observations

[11] Past studies at SP [Davis *et al.*, 2004, 2008; Neff *et al.*, 2008] and Concordia [Legrand *et al.*, 2009] have shown that near-surface chemical concentrations depend significantly on boundary layer meteorological conditions, particularly PBL depth. However, meteorological data over broad reaches of the plateau are very limited. In fact, detailed boundary layer studies focused on the Antarctic plateau have been confined to three widely separated stations: Amundsen-Scott SP Station (SP; 90°S), Concordia Station/Dome C (Concordia; 75°S, 123°E), and Kohlen Station (Kohlen; 77°S, 0°E). Thus, the interpretation of the aircraft data in this study depends on these limited fixed-site data sources and on a combination of meteorological conceptual models of boundary layer flows and recently advanced numerical models.

[12] The conceptual model for surface winds in Antarctica has been dominated over the years by the assumption that these winds are primarily katabatic in origin. Katabatic winds, also referred to as slope winds, arise when a temperature inversion forms over a sloping surface, usually under clear sky conditions. In this model the speed of the wind depends directly on the inversion strength and surface slope, but its direction is modified by the Coriolis effect and friction. However, in the 1970s it was found in experiments at SP that katabatic flows over the interior are also modulated by large-scale weather patterns so that light-wind/strong-temperature inversion conditions, which would tend to lead to shallow boundary layers, occur only intermittently as reported by Neff [1999]. Such modified katabatic conditions with light surface winds typically alternate (e.g., days to weeks) with periods of high winds, warmer temperatures, and overcast skies. Under the latter conditions, weaker/deeper inversions are formed as the warm air adjusts to the colder snow surface. Thus, changing large-scale weather patterns can provide one of the components necessary to explain the continually shifting chemical environments experienced at SP and other sites on the plateau.

[13] As shown in Figure 1 the ANTICI flight paths for flights 5–7 lie over the portion of the plateau that is between SP and Concordia. During the time period covered by these flights the only routine rawinsonde soundings on the plateau were those from SP and Concordia. Complementing these continuously operating stations, however, were the automatic weather stations (AWS) at Concordia (i.e., University of Wisconsin: <http://uwamrc.ssec.wisc.edu/index.html>), Dome A (80.4°S, 77.5°E; operated jointly by China and the Australian Antarctic Division: <http://www.aad.gov.au>), and Midpoint (75°S, 145°E; Programma Nazionale di Ricerche in Antartide (PNRA): <http://www.climantartide.it>). Between these fixed points no meteorological data were available. Consequently, within the limitations defined by the 1 min averaging of the aircraft data, the resulting profiles for NO along with temperature provided the only direct estimate of PBL depth and inversion strength. These estimates, in turn, provided the basis for a comparison with numerical model predicted values. (Note that since the ascent/descent rate of the aircraft varied from 10 to 50 m/min, the temperature data were averaged to 1 min to be commensurate with the averaging time required for the NO observations.)

[14] As one indication of the surface meteorological conditions most likely encountered during ANTICI flights, Figure 2 summarizes conditions on the high plateau as reported by different AWS located near the southern and northern extremes of the ANTICI 2005 flight tracks (i.e., SP, Concordia, Dome A, and Midpoint). While both SP and Midpoint (Figures 2a and 2b) show relatively high winds during flights 5–7 and 10, Concordia (Dome C) and Dome A (Figures 2c and 2d) show much lighter winds. Figure 2 also reveals that diurnal cycling in both temperature and wind speed is evident at Dome A, Concordia, and Midpoint. At Concordia the day-to-night range in temperature is 10°–15°C. At Dome A the diurnal cycle is weaker, but the site is located farther south and at a higher elevation. Midpoint, although at about the same latitude as Concordia, also appears to have a much smaller diurnal temperature cycle during this period. This suggests that latitude alone may not govern the magnitude of the diurnal temperature cycle and, by inference, the development of a convective boundary layer (BL). In contrast, at SP only longer-term synoptically driven changes of 15°C are evident.

[15] During the first series of flights, from 1 to 5 December (flights 5–7), an upper-level high-pressure ridge

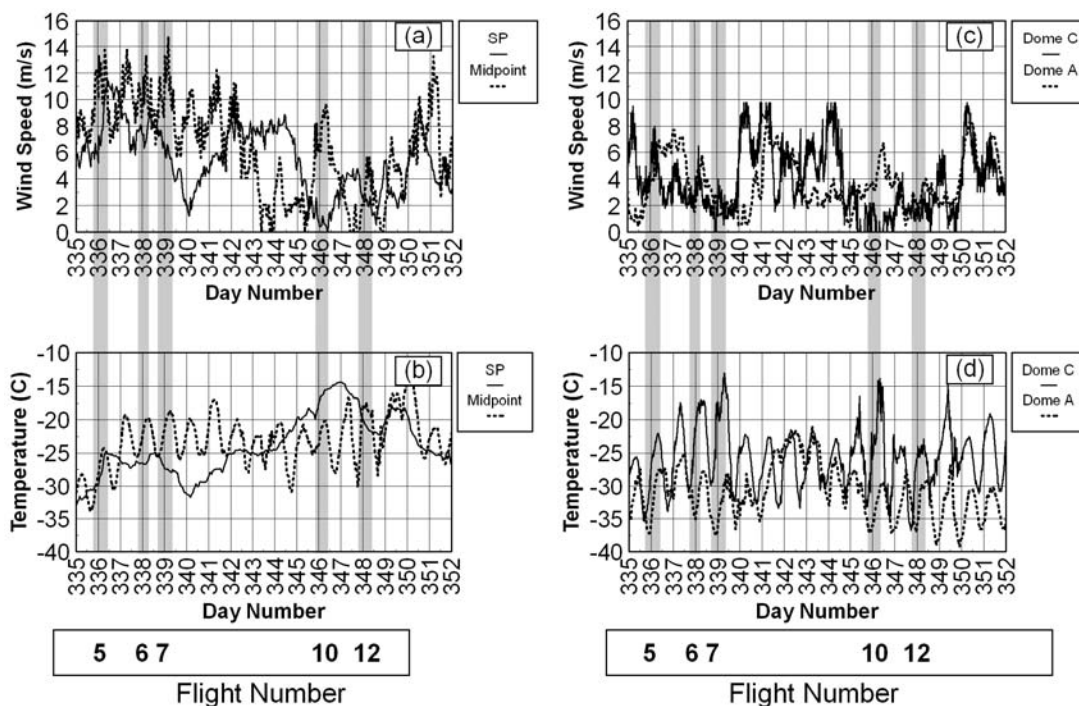


**Figure 2.** (a) Wind speed and (b) temperature at South Pole (SP; solid line) and AWS Giulia (Midpoint; dashed line) and (c) wind speed and (d) temperature from the AWS at Dome C (Concordia; solid line) and Dome A (dashed line) for 1–17 December 2005 (Julian days 335–352). ANTCI flights 5–7, 10, and 12 time periods shown as shaded areas.

had entered the continent from the Indian Ocean, leading to disturbed conditions with high winds at SP ( $>6$  m/s) and rapidly increasing temperatures at Concordia and, later, at SP (Figure 2). Of note, however, is the fact that during the period of high winds at SP, winds at both Concordia and Dome A were rather light. This suggests that a significant variation in surface wind speed occurred along the flight path between these two greatly separated sites, leading to the strong possibility that one might find significantly different chemical environments across the plateau. Normally, high-pressure regions are characterized by subsiding air, which would be consistent with the lowering of the PBL depth at Concordia over the time period of 2–3 December. A rather limited set of sodar profiles from Concordia on 2 December does show a PBL depth of  $\sim 180$  m around local noon; however, by 3 December the daytime depth had dropped to  $\sim 90$  m (S. Argentini, PNRA, personal communication, 2008). Thus, this large-scale meteorological condition of sinking motion may have compensated for the effect of daytime heating and led to a shallower BL.

[16] Further information on meteorological conditions was also obtained from Moderate Resolution Imaging Spectroradiometer (MODIS) satellite imagery (<http://modis.gsfc.nasa.gov/>) and the National Centers for Environmental Prediction (NCEP)/National Center for Atmospheric Research (NCAR) reanalysis [Kalnay et al., 1996] as shown in Figure 3. In Figure 3a the NASA/MODIS cloud product shows partly cloudy to clear conditions as flight 7 approached Vostok. At the start of the flight (not shown) clouds extended from SP to  $87^{\circ}\text{S}$ , which corresponds to the latitude at which the Twin Otter first descended into the BL. North of  $87^{\circ}\text{S}$ , skies were gener-

ally clear. In Figure 3b the NCEP/NCAR reanalysis surface data (available at <http://www.esrl.noaa.gov/psd/>) also show a pattern of light winds over higher elevations of the plateau, with much stronger winds occurring over the Transantarctic Mountains along the Ross Sea. It should be noted that the reanalysis winds in the vicinity of Concordia agree well with the AWS winds shown in Figure 2.

[17] Warming events as shown in Figure 2 also have been noted in the past in conjunction with the advection of significant moisture well into the continent and over the plateau [Sinclair, 1981; van As et al., 2007]. In fact, during the period 1–12 December SP saw one of the highest temperatures on record (e.g.,  $-13.9^{\circ}\text{C}$  on 12 December), compared to a median value of  $-30.1^{\circ}\text{C}$  over the period 1–14 December 1958–2008. Such high temperatures are often associated with increased cloudiness. Historically, for early December the 50 year average cloudiness is 100% when the temperature is higher than  $-20^{\circ}\text{C}$  and 70% for temperatures higher than  $-25^{\circ}\text{C}$ . These conditions at SP are confirmed here as shown in Figure 4, which displays selected temperature profiles together with average daily cloud cover, temperature, and winds. In this case, for profiles on 1 and 3 December the temperature inversion is elevated because of high winds. For the period 6–10 December the base of the inversion layer dropped significantly, to about 100 m, rising again and weakening by 13 December, as the sky became almost totally overcast and surface temperatures warmed dramatically, to higher than  $-15^{\circ}\text{C}$ . During this same period, light and variable surface winds were prevalent over most of the high plateau (Figure 3) as well as aloft (e.g.,  $\sim 1$  m/s at

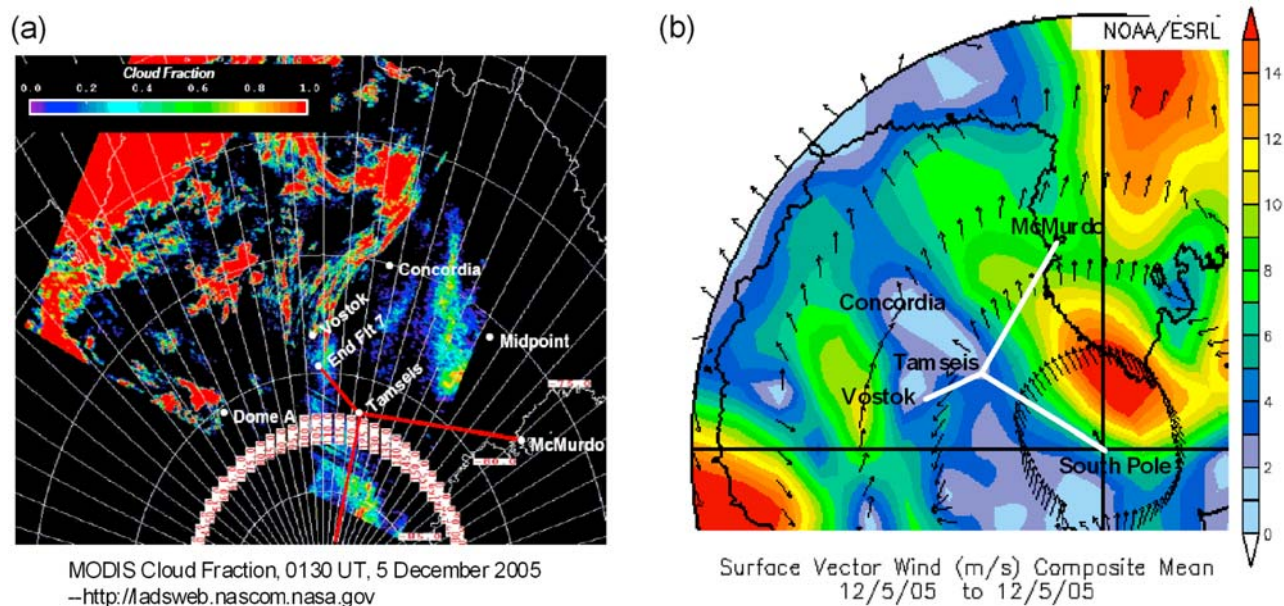


**Figure 3.** (a) MODIS satellite-derived cloud fraction (red, 100%; black, 0%) at the ending time of flight 7 (from <http://ladsweb.nascom.nasa.gov>). (b) NCEP/NCAR reanalysis (from <http://www.esrl.noaa.gov/psd>) surface winds for 5 December 2005. Vectors show wind directions, with color coding indicating wind speed (key at right).

500 hPa on 12–13 December, from rawinsonde data at Concordia).

### 3.3. Meteorological Numerical Modeling Results

[18] Because of the sparse meteorological observations available over Antarctica, the output products from a polar version of the Mesoscale Model version 5 (MM5) [Bromwich *et al.*, 2001; Cassano *et al.*, 2001] were used to gain additional insight into BL behavior over the interior. The use of this model in conjunction with sodar data collected during the 2003 ANTICI field study proved quite useful, resulting in an  $r^2$  correlation coefficient of 0.73 between modeled and observed PBL depth [Wang *et al.*, 2008]. This same model was used to analyze the 2005 data. It has a horizontal spatial resolution of  $80 \times 80 \text{ km}^2$  and contains 27 vertical layers, reaching an altitude corresponding to 10 hPa. Thirteen of these layers are assigned to the lowest 1 km in an effort to simulate the vertical distribution of trace gases in the BL. The four-dimensional data assimilation is based on the European Centre for Medium-Range Weather Forecasts reanalysis, rawinsonde, and surface observations. Most of the meteorological output data were archived every 30 min. Turbulence statistics, however, were archived every 2.5 min to resolve turbulent transport in the BL. The Eta Mellor-Yamada-Janjic (MYJ) 2.5-order closure scheme was used [Black, 1994] for turbulence calculations.

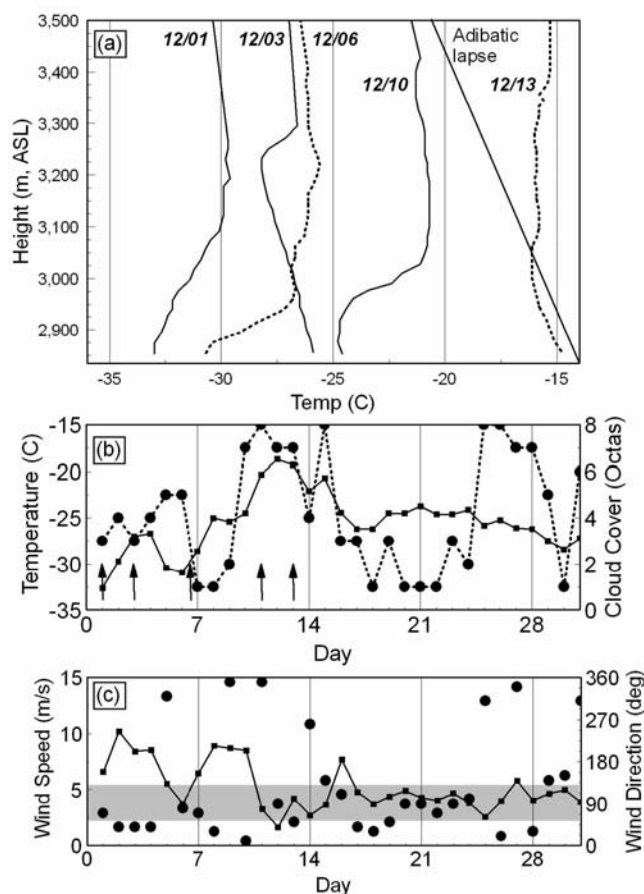
[19] As shown in Figure 5a model products provided the maximum daily PBL depth over the plateau (e.g., Julian day 346, or 5 December) as well as time series plots (Figure 5b) of the daily maximum PBL at specific locations (SP, Vostok, Concordia, and Midpoint) covering the months of November and December 2005. As previously noted these locations were closest to the actual flight tracks for flights 7 and 10. Interestingly, the deeper PBL depths shown in

Figure 5a tend to be coincident with the higher winds in Figure 3b. The individual time series PBL depth profiles also tend to follow the wind speeds indicated in Figure 2, with shallower PBLs coincident with lighter winds at Concordia and Dome A and deeper PBLs at SP and Midpoint, where winds were much higher at the time of flights 7 and 10.

### 3.4. Representative Horizontal Data

[20] Flights 7 and 10 were selected for more detailed analysis from the 2005 study for three reasons: (1) they cover distinctly new, previously unsampled geographical areas, for example, the regions between Tamseis and Vostok and lower portions of the plateau near Midpoint; (2) they provide a contrast between SP, which experiences no diurnal PBL trend, and areas that have a distinct diurnal cycle (e.g., Midpoint); and (3) they each provide significant observations of NO at several altitudes over their respective flight tracks. Flight 7 began at SP and included sampling over some of the highest elevations thus far reached on the plateau (i.e., Vostok) before returning to McMurdo. By contrast, flight 10 was focused southeast of McMurdo Station over a lower-elevation region of the plateau (Midpoint) and a region that experienced diurnal cycling as well as possible intrusions of coastal air.

[21] In Figure 6 time series plots for flight 7 show several relevant chemical, meteorological, and geographical parameters. The flight track indicates that after  $\sim 1.5$  h of flight time ( $\sim 300$  km from SP), the aircraft descended from a radar altitude of  $\sim 600$  m to one of 25 m and reported NO levels of nearly 200 pptv. On the basis of this and subsequent data recordings, a total of eight cases (A–H; Figure 7) have been identified during flight 7 where NO was found to be  $\geq 200$  pptv. For each of these cases the chemical-meteorological



**Figure 4.** (a) South Pole (SP) temperature profiles on 1, 3, 6, 10, and 13 December 2005. (b) Daily average cloud fraction (oktas: solid circles, dashed line) and surface temperature (small solid squares, solid line) for December 2005. Time of temperature profiles indicated by vertical arrows. (c) Daily average wind speed (small solid squares, solid line) and direction (solid circles). Shaded bar: downslope flow directions associated with high NO at SP.

insights gained from the 2003 SP ANTICI study by *Neff et al.* [2008] were utilized in estimating the PBL depth. Using this approach, the radar altitude at which the NO concentration dropped to 50% of the level observed at 25 m (or the lowest altitude sampled) formed the basis for defining the PBL. Although not a meteorologically rigorous methodology for defining the PBL depth, this approach always permitted a relative comparison of the different environments experienced along the sampling track. It is quite encouraging, in fact, that NO and temperature can be seen to vary inversely in Figure 7 as the aircraft descends close to the surface.

[22] Figure 7 also shows that for the flight segment from SP to Tamseis, the aircraft descended into the BL and reached a radar altitude of  $\sim 25$  m on three separate occasions (A–C). After the first descent, each subsequent drop in altitude reveals an increase in temperature both above and within the BL. However, in each of the latter cases the observed level of NO is comparable to that seen during the first descent (200–300 pptv). The average radar altitude over which NO decreased by 50% was in all cases  $\sim 105$  m. The

average temperature change over this same height was  $\sim 1.5^\circ\text{C}$ . Figure 3b shows that along this flight segment, wind speeds were generally in excess of 4 m/s. In terms of surface wind speeds and strength of the temperature inversion, NO concentrations found along this flight were consistent with past observations obtained at the SP in previous campaigns [*Neff et al.*, 2008].

[23] On the segment from Tamseis to Vostok, Figure 3b shows that the aircraft entered a plateau region characterized by light surface winds typically associated in SP studies with highly elevated NO concentrations. As shown in Figure 7 the aircraft started out flying well within the PBL, but this was followed by four ascents/descents (D–G) later in the flight. Each of these systematically shifted the aircraft to a higher geometric elevation. As a result, Figure 7 shows that cooler temperatures with corresponding higher NO levels were encountered. For ascents/descents D and E, after departure from Tamseis, the average PBL is estimated at 82 m and the vertical temperature change over this altitude range is  $2.2^\circ\text{C}$ , suggesting a shallower PBL with a stronger inversion. For descents/ascent F and G, approaching Vostok, the estimated PBL depth is 64 m, and the corresponding temperature change is  $3.6^\circ\text{C}$ . During the latter sequence of events the aircraft was continuing to fly toward Vostok, with NO increasing from 300 to 700 pptv. The highest concentration found during this segment was when the aircraft penetrated a PBL depth of  $\sim 40$  m. (Note that as shown in Figure 3b, the lightest winds ( $< 3$  m/s) are those encountered along the Tamseis-to-Vostok flight segment.) In the last ascent/descent (H) shown in Figure 7 the aircraft was flying from Tamseis back to McMurdo. During this flight leg the PBL depth and temperature are seen to return to values closer to those observed for ascents/descents C and D. Nearly all of the PBL depths estimated directly from the flight 7 aircraft data are generally consistent with the MM5 results displayed in Figure 5a.

[24] As presented in Figure 1 the flight track for flight 10 was configured in the form of a triangle, with both the beginning and the ending sites being McMurdo Station. Only two sides of the triangular flight track were positioned over the plateau; therefore, only these two segments are examined further here. The first leg followed a line from  $159.5^\circ\text{E}$  at 2345 UT to  $145.9^\circ\text{E}$  at 0122 UT, at which point the plane landed at Midpoint to refuel. The second leg began at 0249 UT and followed a line from  $145.9^\circ\text{E}$  back to  $158.8^\circ\text{E}$  at 0417 UT before crossing back over the Transantarctic Mountains. Meteorologically, at around 1500 UT on 11 December (prior to the initiation of flight 10), winds at Midpoint rotated from an initial downslope direction of  $270^\circ$  at 2 to 3 m/s to an upslope direction. By 0400 UT on 12 December they had increased to a speed of 9 m/s. As noted earlier, the model-predicted PBL depth at Midpoint for 12 December (Figure 5b) is consistent with the much higher AWS wind speed data. Both suggest a PBL depth of 200 m or more at Midpoint at the time of sampling.

[25] Time series plots of chemically relevant species for flight 10 are shown in Figure 8. The NO measurements during this flight are interesting in that the highest altitudes reached by the aircraft produced some of the lowest concentrations measured, but the lowest altitudes did not systematically reveal high NO levels the way they did in flight 7. Instead, the NO concentrations covered a wide range of

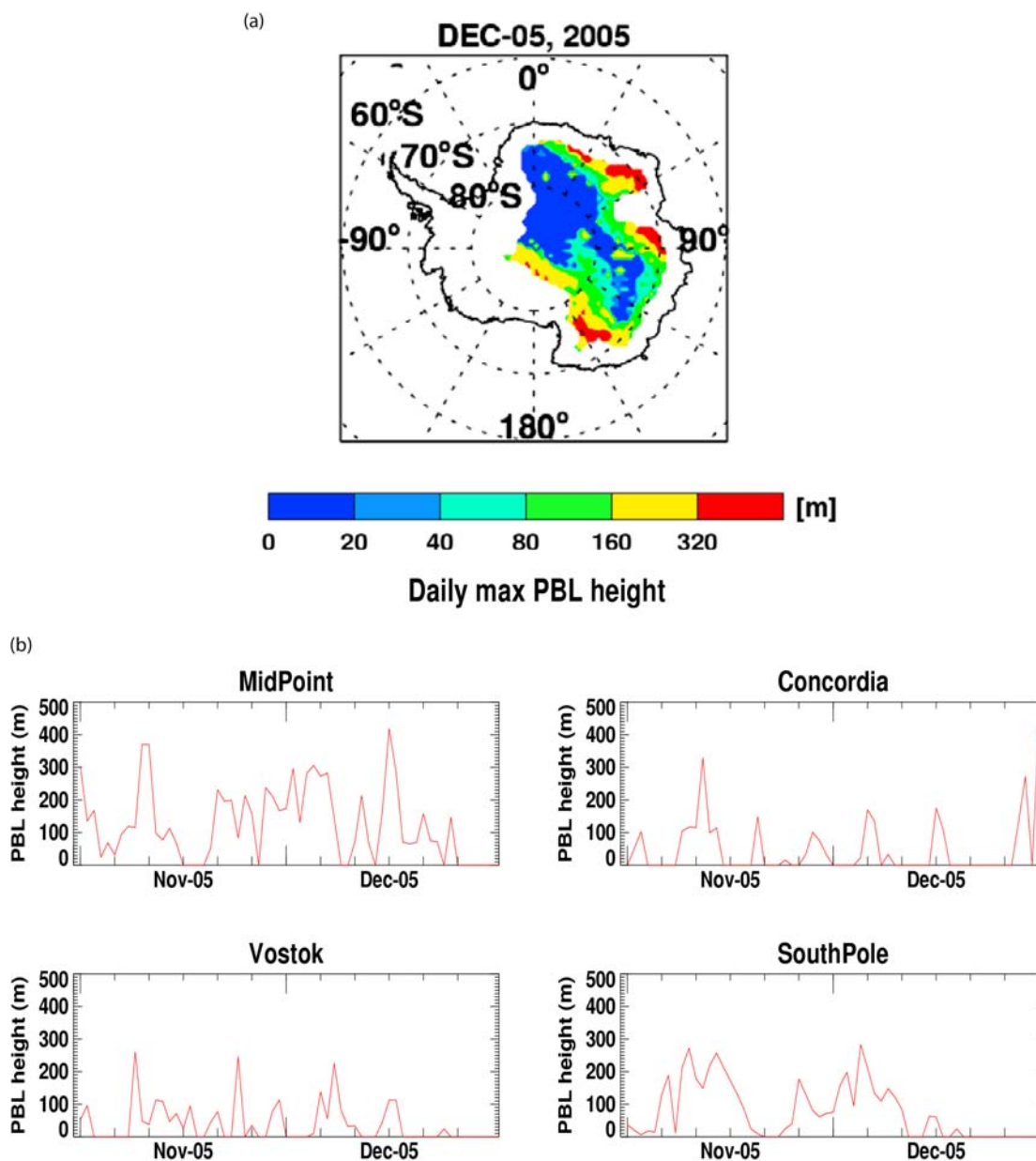


**Figure 5.** Planetary boundary layer (PBL) depths estimated from the polar MM5 simulations. PBL depth is diagnosed based on the falloff of turbulence with height [Wang *et al.*, 2008]. (a) Maximum daily PBL depths over the plateau (e.g., areas above 2000 m) of the Antarctic continent on 5 December. (b) Model-derived time series values of the maximum daily PBL depth at Vostok, Midpoint, Concordia, and SP. Apparent values of zero indicative of very low PBL depths, e.g., <20 m.

values, from very low to modest levels ( $\sim 10$ – $90$  pptv). The correlation between NO and HNO<sub>3</sub> was also found to be much weaker for flight 10 than for flight 7. In fact, early in the first leg of flight 10, the highest HNO<sub>3</sub> levels ( $\sim 100$  pptv) were found at some of the highest sampling altitudes. (See section 4.2.3 for further discussion of this sampling period.) The highly variable levels of NO observed throughout flight 10, especially at low altitudes, suggest that the PBL depth during much of this flight was rather deep, in agreement with the above meteorological analysis.

[26] Photolysis frequencies ( $J_{\text{NO}_2}$ ,  $J_{\text{O}_3}$ ) and temperature are shown in Figures 6 (bottom) and 8 (bottom). (For comparison purposes, the 24 h average  $J_{\text{NO}_2}$  and  $J_{\text{O}_3}$  values at SP at the time of the field study were  $1.15 \times 10^{-2} \text{ s}^{-1}$  and  $1.24 \times 10^{-5} \text{ s}^{-1}$ , respectively.) From these it can be seen that the NO<sub>2</sub> photolysis rate was systematically higher in flight 10 than in flight 7. However,  $J_{\text{O}_3}$  was higher in flight 10 than in flight 7 for only approximately half of the total flight time, being at nearly the same level for the remainder of the sampling period. These results reflect the point made earlier

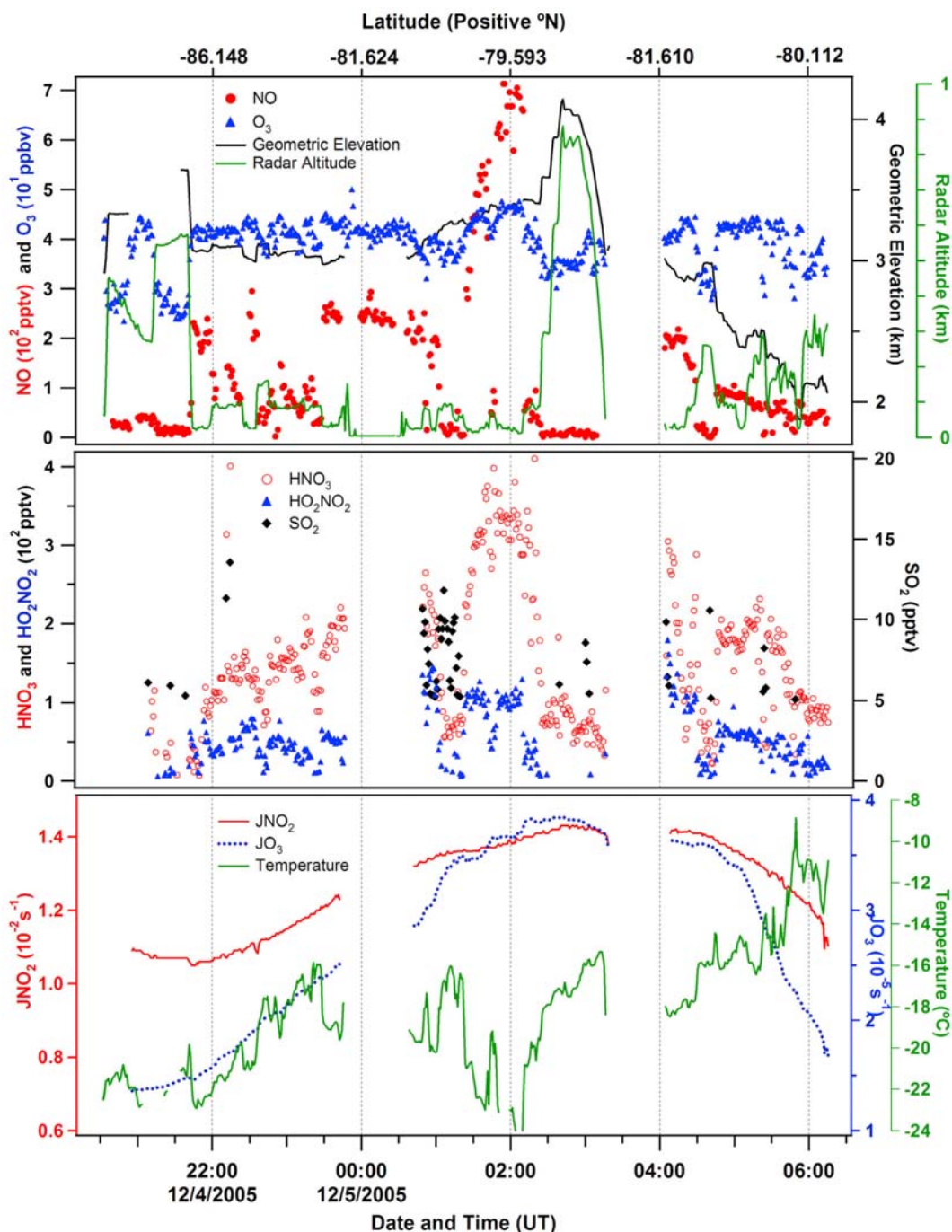


**Figure 6.** Flight 7 time series plot. The top scale indicates the approximate latitude at the time shown on the lower scale (it is not linear). Geometric elevation is referenced to sea level, while radar altitude is referenced to either ground or snow level. (top) NO, O<sub>3</sub>, geometric altitude, and radar altitude. (middle) HNO<sub>3</sub>, HO<sub>2</sub>NO<sub>2</sub>, and SO<sub>2</sub>. (bottom)  $J(\text{NO}_2)$ ,  $J(\text{O}^1\text{D})$ , and temperature. All data have been averaged for 1 min. Dates are given as month/day/year.

regarding diurnal solar cycling being a significant factor in flight 10 relative to SP and more centrally located sites. Not surprisingly, the air temperature profiles shown for flights 7 and 10 are a reasonably good reflection of the geometric elevation differences between these two flights. In the case of flight 7 the temperature range was  $-24.3^\circ\text{C}$  to  $-8.9^\circ\text{C}$ , with an average of  $-18.2^\circ\text{C}$ . The range for flight 10 was

somewhat smaller,  $-20.0^\circ\text{C}$  to  $-13.6^\circ\text{C}$ , with an average of  $-17.2^\circ\text{C}$ .

### 3.5. Vertical Profiles

[27] A useful characteristic of aircraft field sampling is the ability to record data at many different altitudes. This allows for the development of vertical profiles of chemical species,

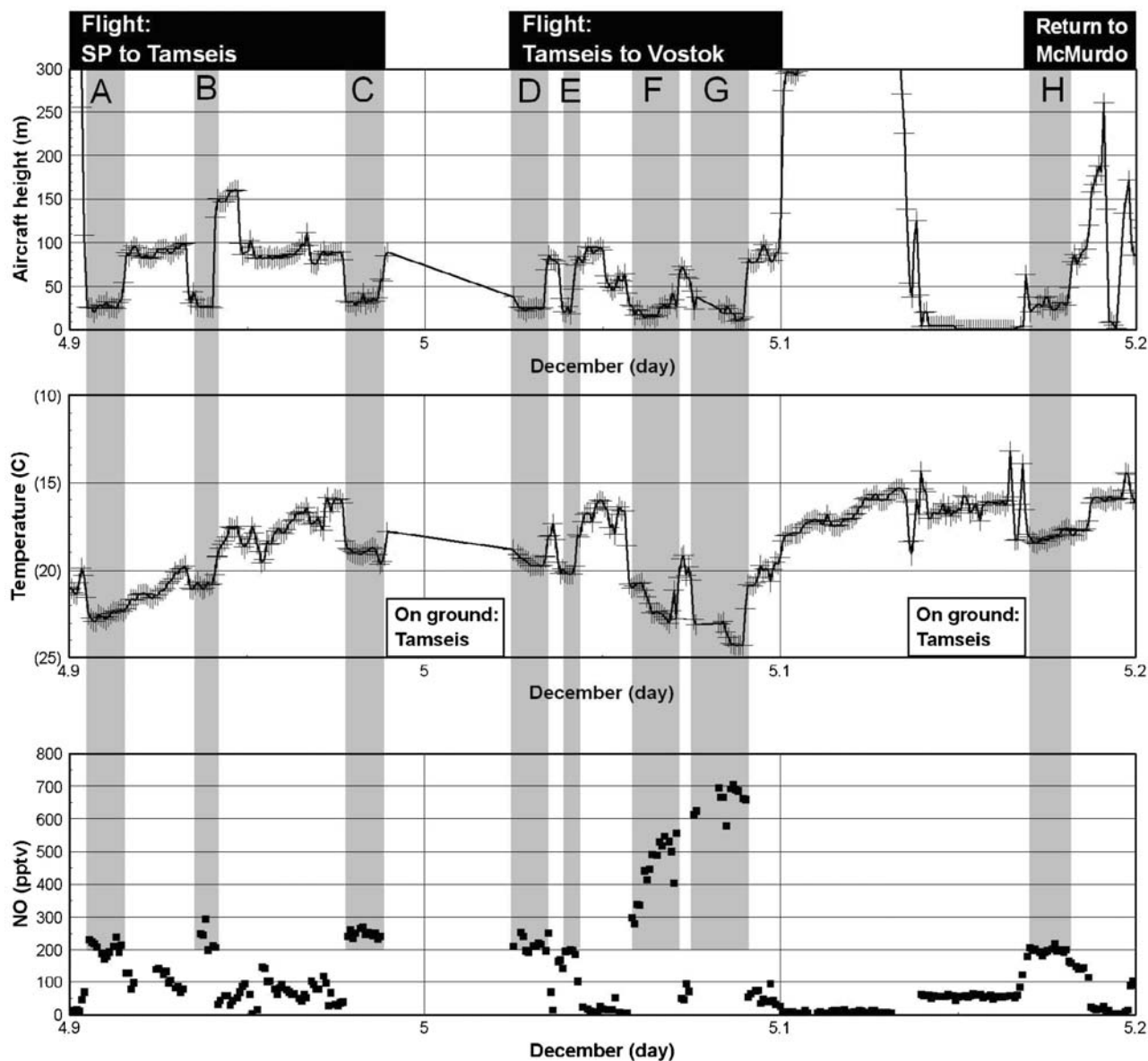


**Figure 7.** Flight 7: (top) aircraft radar altitude, (middle) temperature, and (bottom) NO along flight track from SP to Tamseis and then to Vostok, returning to McMurdo. Descents into the boundary limit where NO > 200 pptv are shown by shading.

which are especially helpful in distinguishing surface sources from in situ production or long-range transport. In Figure 9 the vertical distributions for several of the more critical trace gases measured during ANTCI 2005 are presented. These include NO (Figure 9a), O<sub>3</sub> (Figure 9b), HNO<sub>3</sub> (Figure 9c), HO<sub>2</sub>NO<sub>2</sub> (Figure 9d), SO<sub>2</sub> (Figure 9e), and water vapor (i.e., dew point (Figure 9f)).

[28] Figures 9a, 9c, and 9d reveal that with the possible exception of flight 10, the nitrogen oxide species NO, HNO<sub>3</sub>, and HO<sub>2</sub>NO<sub>2</sub> all follow a similar trend of decreasing concentration with increasing radar altitude. For flight 10, as mentioned earlier, the average PBL depth was considerably deeper than for the other four flights. In fact, the scatter in the low-altitude NO data makes it difficult even to assign a PBL value from the aircraft data, thus relegating its

estimation to the output provided by the polar MM5 (i.e.,  $\geq 200$  m). Given the latter estimate, it is not surprising that both HNO<sub>3</sub> and HO<sub>2</sub>NO<sub>2</sub> follow a trend similar to that for NO: invariance in concentration levels with increasing altitude. The vertical profiles for ozone (Figure 9b), with the exception of flight 10, also reveal a general trend of decreasing concentration with increasing radar altitude. Thus, these data are consistent with the altitude trend data previously recorded at SP [Crawford *et al.*, 2001; Helmig *et al.*, 2008a; Johnson *et al.*, 2008].

[29] Of the six vertical concentration profiles shown in Figure 9, only the one for SO<sub>2</sub> shows no evidence of an altitudinal trend. Indications are that it is relatively well mixed throughout the lower 1 km of the plateau's atmosphere. The only possible exception to this generalization

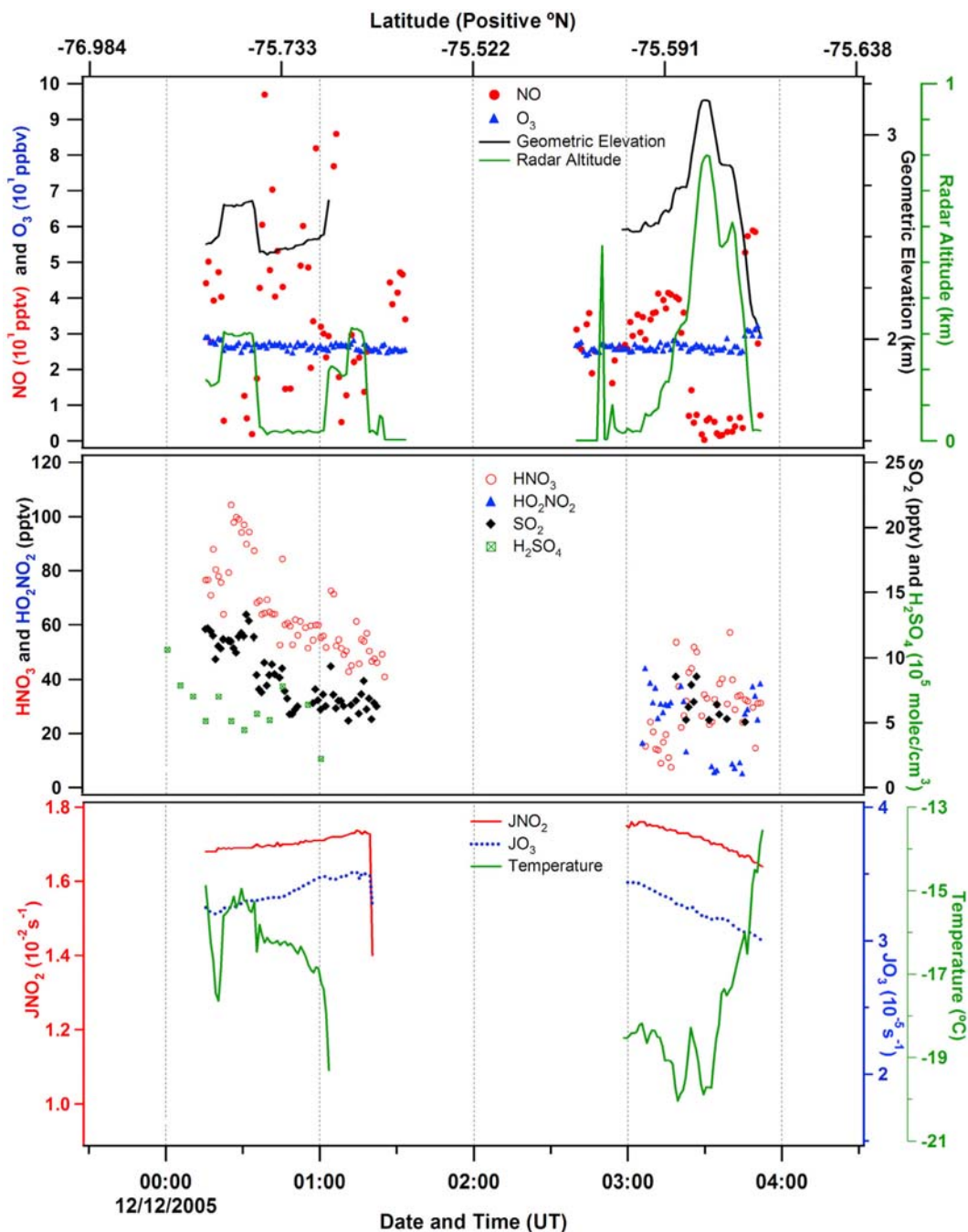


**Figure 8.** Flight 10 time series plot. The top scale indicates the approximate latitude at the time shown on the lower scale (it is not linear). Geometric elevation is referenced to sea level, while radar altitude is referenced to either ground or snow level. (top) NO, O<sub>3</sub>, geometric elevation, and radar altitude. (middle) HNO<sub>3</sub>, HO<sub>2</sub>NO<sub>2</sub>, SO<sub>2</sub>, and H<sub>2</sub>SO<sub>4</sub>. (bottom)  $J(\text{NO}_2)$ ,  $J(\text{O}^1\text{D})$ , and temperature. All data have been averaged for 1 min except for H<sub>2</sub>SO<sub>4</sub>, which has been averaged for 5 min.

again involves flight 10. A close inspection of Figure 8 shows that early in this flight (after reaching the lower edges of the plateau), there is an apparent trend in SO<sub>2</sub> as a function of radar altitude (for further detail see the discussion in section 4.2.3). As stated above, however, the vertical distribution for SO<sub>2</sub> shows little evidence of a local surface source for this species. A similar conclusion can be reached regarding the trace gases CO, ethane, ethyne, and the halocarbon methyl chloroform (see Figure 10), as none

of these shows evidence of a significant vertical trend in concentration.

## 4. Discussion

### 4.1. General Overview

[30] As stated earlier the major goal of this study was to determine whether the numerous NO events observed at SP, and the ensuing chemistry, are representative of the larger

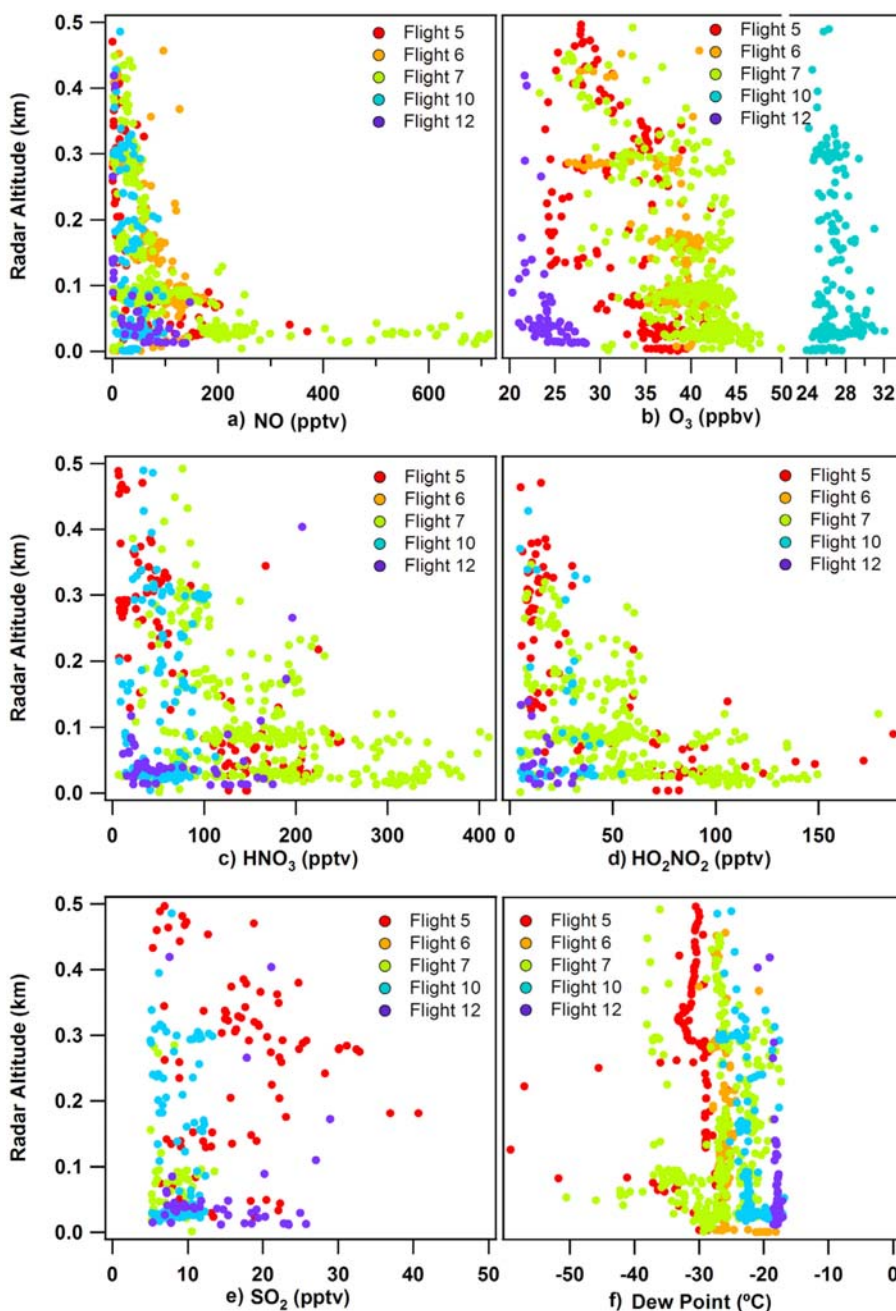


**Figure 9.** Vertical profiles for (a) NO, (b) O<sub>3</sub>, (c) HNO<sub>3</sub>, (d) HO<sub>2</sub>NO<sub>2</sub>, (e) SO<sub>2</sub>, and (f) dew point, all color-coded by flight number. Overall, 74% of plateau data were recorded at radar altitudes of  $\leq 0.5$  km. Two outlier points for SO<sub>2</sub> are not shown. Also, data below the 5 pptv detection limit for SO<sub>2</sub> during ANTCI 2005 are omitted.

plateau. The degree to which this was found to be true is the principal topic of discussion in section 4.2. Section 4.3 is devoted to providing the meteorological evidence that further supports these chemical findings.

#### 4.2. Comparison of SP Ground-Based Chemical Data With Airborne Results

[31] Although the atmospheric level of NO clearly represents the most important criterion for comparing the SP chemical environment with that found over vast stretches of the plateau, the trends in related chemical species also

provide a basis for quantitative comparison. For this reason, the concentrations of HNO<sub>3</sub>, HO<sub>2</sub>NO<sub>2</sub>, and O<sub>3</sub> are also explored below.

##### 4.2.1. NO

[32] A summary of median values for NO recorded in different years is presented in Table 3. The airborne data there are given for three altitude ranges, while those recorded at SP are for a sampling elevation  $\sim 10$  m above the snow's surface. Also provided in Table 3 are median concentrations of chemically coupled species such as HNO<sub>3</sub>, HO<sub>2</sub>NO<sub>2</sub>, and O<sub>3</sub> as well as the levels of several noncoupled

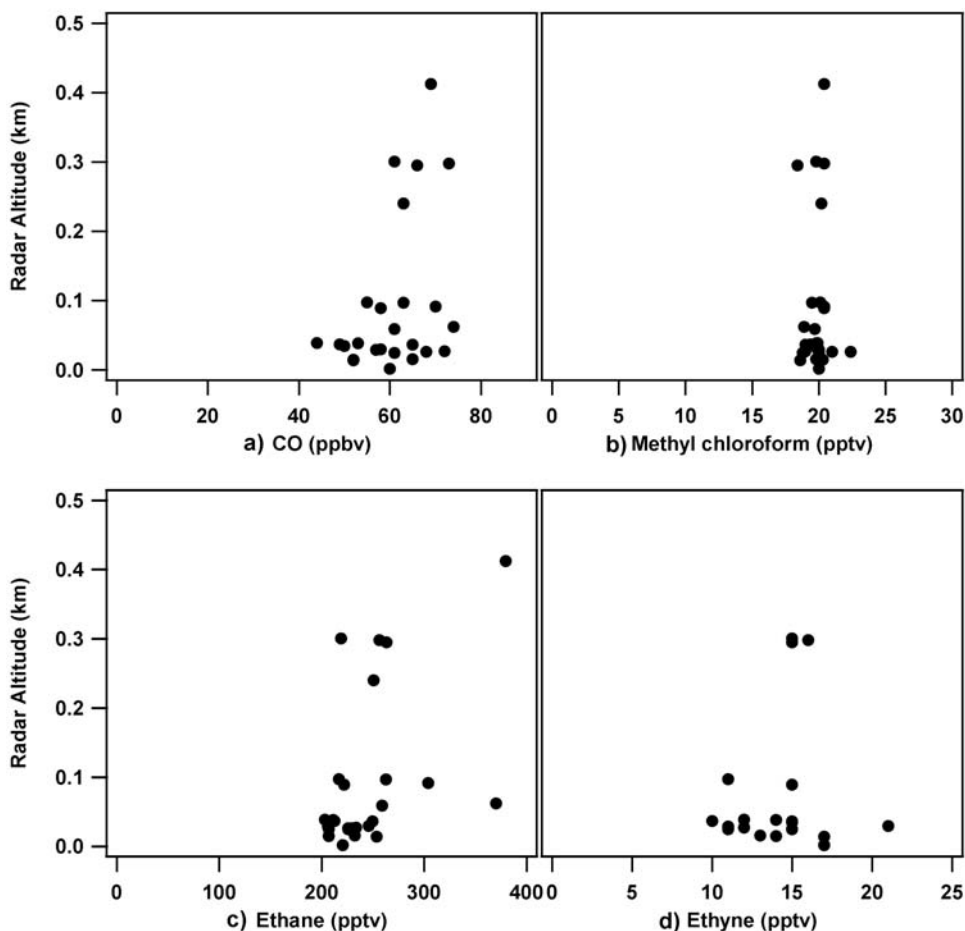


**Figure 10.** Vertical profiles for (a) CO, (b) methyl chloroform, (c) ethane, and (d) ethyne. Overall, 74% of plateau data were recorded at radar altitudes of  $\leq 0.5$  km. One outlier point for CO is not shown.

species. In each case, the data are those recorded over the calendar period of 1–15 December, thus overlapping the sampling period for ANTICI flights 5–7, 10, and 12. SP results from the year 1998 are listed first in Table 3 since that is the first year in which direct observations of NO were recorded at this site. Subsequent sampling years include 2000, 2003, and 2006. Only the 2006 data have not yet been published.

[33] From Table 3 it can be seen that SP NO median values for the years 1998, 2000, 2003, and 2006 are 209, 82, 164, and 149 pptv, respectively. The near-surface median NO level for the limited 2003 airborne results (not listed in Table 3) was 250 pptv, a value that exceeds the highest median estimated for SP. For comparison, the near-surface 2005 airborne data (i.e., data recorded between 0 and 50 m) show a median value of 95 pptv. However, if the observa-

**Table 3.** Median Concentrations of Trace Gases for South Pole and Other Plateau Sites<sup>a</sup>

Parameter	SP ARO				ANTICI 2005 Airborne <sup>b</sup>		
	ISCAT 1998 <sup>c</sup>	ISCAT 2000 <sup>c</sup>	ANTICI 2003 <sup>c</sup>	ANTICI 2006	0–50 m	51–150 m	151–500 m
NO (pptv)	209	82	164	149	95 (140) <sup>d</sup>	90	30
O <sub>3</sub> (ppbv)	33	35	32	30	36	40	33
HNO <sub>3</sub> (pptv)		18 <sup>e</sup>	63		120	140	64
HO <sub>2</sub> NO <sub>2</sub> (pptv)			42		64	42	21
SO <sub>2</sub> (pptv)		5	10		10	9	12
CO (ppbv)		37	46	62	59	62	66
CH <sub>3</sub> CCl <sub>3</sub> (pptv)		48 <sup>f</sup>	25 <sup>f</sup>	15	20	20	20
C <sub>2</sub> H <sub>6</sub> (pptv)	417	180	188	220	223	261	256
C <sub>2</sub> H <sub>2</sub> (pptv)		22 <sup>f</sup>	14 <sup>f</sup>	20	14	13	15

<sup>a</sup>Abbreviation: ARO, Atmospheric Research Observatory.

<sup>b</sup>Airborne median values from ANTICI 2005 are from plateau flights shown in Figure 1 (i.e., flights 5–7, 10, and 12).

<sup>c</sup>Values from 1 to 15 December in Table 3 of Eisele et al. [2008] unless otherwise noted.

<sup>d</sup>Median value after removal of flight 10.

<sup>e</sup>Value from 15 to 31 December in Table 3 of Eisele et al. [2008].

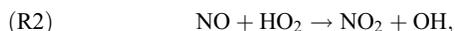
<sup>f</sup>Previously unpublished.

tions from flight 10 are removed, the airborne median increases to 140 pptv. (Recall that the estimated PBL depths encountered during flight 10 were quite deep.) Thus, given the natural year-to-year variability in NO, these results make the case that the airborne data are generally consistent with those recorded at SP. More specifically, they suggest that highly elevated levels of NO are a common feature of large areas of the plateau during the austral spring/summer time period. Speculation here is that this is very likely a common chemical characteristic over the entire plateau region as defined in Figure 1.

[34] The ANTICI 2005 data shown in Figure 9 also support the conclusion that the source of NO is snow photochemistry. In particular, Figure 9 shows a systematic decrease in NO as a function of altitude, a trend that would be expected if NO<sub>x</sub> were being photochemically released from the surface snow layer. This same trend has also been reported for the SP site on several occasions [see, e.g., Davis *et al.*, 2004, 2008; Helmig *et al.*, 2008b; Neff *et al.*, 2008; Oncley *et al.*, 2004].

#### 4.2.2. O<sub>3</sub>, HNO<sub>3</sub>, and HO<sub>2</sub>NO<sub>2</sub>

[35] Given the strong chemical coupling between NO<sub>x</sub> and HO<sub>x</sub> (OH + HO<sub>2</sub>) chemistry, it is reasonable to expect a significant correlation among the various species involved. If demonstrated to be true, this provides yet another confirming test of chemical commonality between the plateau and SP. The most obvious species involved in the NO<sub>x</sub>-HO<sub>x</sub> chemical system include OH, HO<sub>2</sub>, O<sub>3</sub>, NO<sub>2</sub>, HNO<sub>3</sub>, and HO<sub>2</sub>NO<sub>2</sub>. Of these, extensive observations are now available only for O<sub>3</sub>, HNO<sub>3</sub>, and HO<sub>2</sub>NO<sub>2</sub>. In the case of O<sub>3</sub> earlier SP investigations have been reported by Crawford *et al.* [2001], Helmig *et al.* [2008a], and Oltmans *et al.* [2008]. The relevant chemical reactions are summarized here:

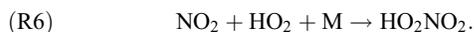
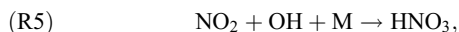


From these it follows that each time an NO molecule is converted to NO<sub>2</sub> via (R2), a corresponding O<sub>3</sub> molecule must also be produced via (R3) and (R4). When this rate exceeds the rate of photochemical destruction of O<sub>3</sub>, a prevalent summertime plateau condition, net photochemical production of O<sub>3</sub> results [Chen *et al.*, 2004; Crawford *et al.*, 2001; Helmig *et al.*, 2008a]. Because the cycling time for these reactions is on the order of minutes, the expectation is that the concentration trends in NO should be mirrored in O<sub>3</sub>. However, as reported in Table 3 the SP data for NO and O<sub>3</sub> show little evidence of this trend. A comparison of the levels of NO and O<sub>3</sub> in the time series plot for flight 7 (e.g., Figure 6; 0100–0200 and 0400–0430 UT), as well as those shown for NO and O<sub>3</sub> in the vertical profile plots in Figures 9a and 9b, is far more encouraging. In both cases, there is a general trend of elevated O<sub>3</sub> levels coincident with elevated NO levels. The fact that the level of correspondence between the two species is not greater is primarily a reflection

of the difference in their respective lifetimes. Under plateau conditions O<sub>3</sub> has a lifetime of months versus <1 day for NO<sub>x</sub>. Thus, even though both have sinks in the atmosphere, the much longer lifetime of O<sub>3</sub> means that it can also be modulated by atmospheric transport processes, thereby somewhat masking its local photochemical production. The latter impact is accentuated in the statistically massaged SP data reported in Table 3.

[36] An interesting consequence of the plateau O<sub>3</sub> chemistry cited above is that in one of the most pristine areas of the world, local photochemistry is a major source of O<sub>3</sub> during the spring/summer months. This conclusion was first drawn from the SP study carried out in 1998 as reported by Crawford *et al.* [2001]. More recently, these earlier results have been greatly expanded on in studies reported by Helmig *et al.* [2008a] and Oltmans *et al.* [2008] at SP and by Legrand *et al.* [2009] at Concordia, Antarctica.

[37] Both HNO<sub>3</sub> and HO<sub>2</sub>NO<sub>2</sub> share a common chemical characteristic with O<sub>3</sub> in that their production requires that NO first be oxidized to NO<sub>2</sub>. This process is followed by (R5) and (R6):



Since the times for conversion of NO to NO<sub>2</sub> (minutes) and for oxidation of NO<sub>2</sub> to HNO<sub>3</sub> or HO<sub>2</sub>NO<sub>2</sub> (7–20 h) are relatively short, the degree of correspondence between these end products and NO might again be expected to be relatively high, provided that their removal times are also relatively short. However, unlike O<sub>3</sub>, the removal process for these two species is more complex. Evaluating their lifetimes requires reliable values for the surface scavenging efficiencies and the rate at which these species are transported to the snow surface. There are presently significant uncertainties in both. Close to the snow's surface (i.e., within several meters), physical scavenging has been estimated to occur with high efficiency, resulting in lifetimes as short as 0.5 days [Slusher *et al.*, 2002]. However, transport times to the surface are a strong function of atmospheric stability. Therefore, the mixing time within the PBL is a critical factor in defining the lifetimes of HNO<sub>3</sub> and HO<sub>2</sub>NO<sub>2</sub> [Wang *et al.*, 2008]. The greater the distance from the snow's surface, the longer the expected lifetime with respect to deposition. It follows that the lifetimes for these species can be significantly enhanced above the PBL. In the case of HNO<sub>3</sub>, its lifetime will nearly always exceed that for NO<sub>x</sub>. Under these conditions, HNO<sub>3</sub> levels will also tend to be influenced by transport processes.

[38] Adding complexity to the determination of the lifetime of HO<sub>2</sub>NO<sub>2</sub> is the additional removal of this species from the atmosphere by both photochemical processes and thermal dissociation [Gierczak *et al.*, 2005; Jiménez *et al.*, 2004, 2005]. Though the uncertainties associated with these two loss processes are sizable, their impact is still that of reducing further the lifetime of HO<sub>2</sub>NO<sub>2</sub>. Thus, this species should also reveal a significant correlation with NO.

[39] The ISCAT data set in Table 3 provides an opportunity to examine the degree of correlation between HNO<sub>3</sub> and NO at SP. Unfortunately, the first HNO<sub>3</sub> measurements

in the year 2000 were made only during the last 2 weeks of December. Though lacking statistical rigor, a comparison of NO with HNO<sub>3</sub> was still undertaken after establishing that the median NO value for weeks 1 and 2 of December was essentially the same as that for weeks 3 and 4, i.e., 82 and 88 pptv, respectively [Eisele *et al.*, 2008]. As a result, it was assumed that the median level of HNO<sub>3</sub> for weeks 1 and 2 was most likely similar to the value estimated from weeks 3 and 4. With this approximation the year 2000 final median concentrations for HNO<sub>3</sub> and NO are reported as 18 and 82 pptv, respectively. These can be compared to the 2003 SP medians of 63 and 164 pptv, respectively. Collectively, these SP results support the idea that HNO<sub>3</sub> is chemically coupled to NO as previously reported by Davis *et al.* [2008] based on a more rigorous statistical analysis of higher-resolution data. However, the more relevant question is how consistent these SP results are with those recorded during the ANTCI 2005 airborne study.

[40] As discussed above, an important aspect of the airborne data is the fact that once a radar altitude of a few tens of meters is exceeded (e.g., when above the PBL), the lifetime of HNO<sub>3</sub> can be significantly extended. More specifically, it becomes a strong function of both the PBL depth and the mixing rate of the atmosphere. For the altitude range 0–50 m, Table 3 shows that the 2005 airborne data result in a median concentration of 95 pptv for NO, whereas that for HNO<sub>3</sub> is 120 pptv. Removal of flight 10 data based on the earlier discussion of the uniqueness of this flight, however, shifts the NO median up to 140 pptv, with only a small increase in HNO<sub>3</sub>. Concentrations of both species are also elevated in the 51–150 m (90 pptv NO, 140 pptv HNO<sub>3</sub>) and 151–500 m (30 pptv NO, 64 pptv HNO<sub>3</sub>) altitude bins. For these higher-altitude bins (frequently above the PBL), the enhanced lifetime of HNO<sub>3</sub> versus that of NO<sub>x</sub> is apparent.

[41] Yet another method of assessing the degree of chemical coupling between HNO<sub>3</sub> and NO is provided by the real-time flight data. This can be seen in the concentration-versus-altitude plots in Figures 9a and 9c. In these plots the general trend in both NO and HNO<sub>3</sub> is clearly one of decreasing concentration with increasing altitude, as would be expected if the two species are chemically coupled and both are reasonably short-lived. The minute-by-minute airborne data shown in Figure 6 are equally convincing. There the correlation between NO and HNO<sub>3</sub> resulted in  $r^2 = 0.5$ , which is one of the highest values for any two airborne chemical variables tested.

[42] Turning to the species HO<sub>2</sub>NO<sub>2</sub>, it can be expected that with a lifetime shorter than that of HNO<sub>3</sub> this would result in an increasing HNO<sub>3</sub>:HO<sub>2</sub>NO<sub>2</sub> ratio with increasing altitude. This point is illustrated in Table 3, where the ratio is ~2:1 for the altitude bin of 0–50 m and closer to 3:1 for the 51–150 and 150–500 m bins. By analogy, the HO<sub>2</sub>NO<sub>2</sub> data also support the idea that there is strong chemical coupling with NO, as first demonstrated in the ground-based 2003 SP study [Davis *et al.*, 2008].

#### 4.2.3. Other Species

[43] As reported in Table 3 and in Figure 10, for those species having no known chemical pathway coupling them to NO, no evidence suggesting otherwise was found in the ANTCI 2005 data. This also was found to be the case for data previously collected at SP. Species falling into this category include SO<sub>2</sub>, CO, CH<sub>3</sub>CCl<sub>3</sub>, C<sub>2</sub>H<sub>6</sub>, and C<sub>2</sub>H<sub>2</sub>.

However, when the comparison species is switched from NO to HNO<sub>3</sub>, an exception appears. The exception involves SO<sub>2</sub> recorded during flight 10, as shown in the time series plot in Figure 8. From 0015 to 0120 UT,  $r^2 = 0.72$  for the correlation between SO<sub>2</sub> and HNO<sub>3</sub>. For all other chemical data collected over the plateau during the 2005 study, no correlation was found. The latter finding also holds true for data collected over nearly all coastal sites, the one exception being those flights focused on the Mount Erebus volcanic plume (flights 8 and 9).

[44] During flights 8 and 9, which sampled the Mount Erebus plume, the  $r^2$  correlation between SO<sub>2</sub> and HNO<sub>3</sub> reached 0.9 [Oppenheimer *et al.*, 2010]. Supporting this trend in SO<sub>2</sub>, Figure 8 also shows a limited set of observations of the SO<sub>2</sub> oxidation product H<sub>2</sub>SO<sub>4</sub>. These data clearly track the profile of SO<sub>2</sub> early in the flight. However, in an effort to provide additional evidence relating the flight 10 observations to Mount Erebus emissions, forward air trajectory analyses were performed using the output from the previously discussed polar MM5. The results strongly suggest that the atmospheric chemical composition observed in the early stages of flight 10 was influenced by the Mount Erebus plume. Since this volcano is approximately 600 km WSW of the point of sampling, we estimate that the plume was likely airborne for 3 to 4 days before being intercepted by the Twin Otter. This Erebus plume encounter over the plateau appears to be one of the first recorded cases where both HNO<sub>3</sub> and SO<sub>2</sub> have been measured simultaneously. Thus, it defines an important new piece of evidence pointing toward the impact of Mt. Erebus emissions on trace chemicals in Antarctic plateau snow. (For further details regarding the Mount Erebus volcano study, see Oppenheimer *et al.* [2010].)

[45] The ANTCI 2005 data also provide insight into the issue of DMS as a potential source of plateau SO<sub>2</sub>. At very low temperatures DMS is oxidized by either OH or BrO to form predominantly the intermediate species dimethylsulfoxide (DMSO), which under low aerosol conditions typically forms SO<sub>2</sub>. During the ANTCI plateau flights the measured levels of DMS were extremely low at all altitudes. Most measurements, in fact, were at or below the detection limit of 1 pptv. Considering the large amounts of DMS that are typically emitted into the atmosphere each spring/summer season from coastal waters surrounding Antarctica, this suggests that most SO<sub>2</sub> reaching the plateau is formed close to its ocean source. The possibility of some contribution from still more distant sources, however, cannot be totally excluded.

#### 4.3. Vertical Mixing: Effects of Latitude and Topography on Chemical Distributions

[46] The earlier analysis of meteorological and aircraft observations, particularly during flight 7, paints a relatively consistent picture of PBL depths that were largely controlled by meteorological conditions, particularly as influenced by wind speed and location on the plateau. In the absence of disturbed weather conditions, PBL depths and NO concentrations were found to be similar to those previously observed at SP. In particular, clear skies and light wind speeds were coincident with shallow PBLs (e.g., flight 7, Tamseis to Vostok), where values of NO exceeding 300 pptv were typically found at altitudes below 40 m. These values

are comparable to some of the higher values recorded in past field studies carried out at SP. The shallow PBLs inferred from the aircraft profiles were also confirmed in model calculations.

[47] Shallow, katabatic winds, as described by *Neff et al.* [2008], can also play a key role in confining snow emissions close to the surface. An aspect of these katabatic flows important to the generation of high NO concentrations is the presence of a low-level wind speed maximum that is some tens of meters above the surface yet moving at high speeds. This condition tends to confine surface emissions below the height at which the maximum speed occurs. Thus, an important question that has surfaced during this study is how to assign the relative importance of katabatic winds and diurnal cycling effects on the PBL depth northward from SP. Past BL studies at SP, Concordia, and Kohnen shed some light on this question. For example, in contrast to the shallow PBLs typically found at SP, the presence of solar cycling at Concordia appears to produce significant diurnal changes in the PBL [*Legrand et al.*, 2009]. At night a shallow inversion develops, but during daylight hours the PBL can increase to several hundred meters as driven by sensible heating [*King et al.*, 2006]. As noted earlier, sodar data from Concordia on 2–3 December 2005 were consistent with the predictions of *King et al.* [2006] in that significant mixing was observed but may have been reduced somewhat by a large-scale sinking motion associated with a high-pressure ridge aloft. Similarly, limited summertime results from Kohnen Station, at approximately the same latitude as Concordia (see Figure 1), reveal little evidence of deep mixing, a typical PBL depth being ~70 m. A partial answer to this riddle seems to be that even though both experience diurnal cycles, the persistence into daytime of a nocturnal low-level katabatic jet associated with the local topography at Kohnen significantly reduces an otherwise deeply mixed BL that would normally develop from diurnal heating. In fact, the latter behavior has even been simulated with a high-resolution, one-dimensional numerical model [*van As et al.*, 2006, 2007]. Thus, these results suggest that in katabatic regions away from SP, such as those probed during flights 5–7, the development of a convective BL can be inhibited compared to that on elevated domes like Concordia. A detailed probing of the BL during flight 7 (Figure 7) supports this conclusion in revealing that even under clear sky conditions (Figure 3b), very shallow PBLs, similar to those at SP, can develop despite the presence of a solar diurnal cycle. These results suggest, then, that factors other than Sun angle and wind speed can influence the daily course of temperature and vertical mixing and are worthy of future study.

[48] A final element of this investigation of factors that influence PBL depths involves sampling efforts on the fringes of the plateau, where both topography and possible intrusions of marine air might be significant. The airborne 2005 data clearly show systematically higher levels of NO, as well as O<sub>3</sub>, in the interior regions of the plateau than near the fringes. For flights 10 and 12, in particular, the areas sampled experienced higher Sun angles and also were closer to the coast. As discussed earlier, the time series plot for NO during flight 10 (Figure 8) clearly shows much lower average values for NO and also reveals far greater variability

in levels, particularly during sampling at low altitudes. Although the limited sampling time in these fringe areas could be presenting an atypical picture, speculation here is that the results reflect diurnal cycling effects in combination with more variable wind directions and transport paths into these areas.

## 5. Summary and Conclusions

[49] Based on flight path coverage which involved approximately 8000 km of plateau terrain, we estimate that between the ANTCI 2003 and the ANTCI 2005 airborne studies, the area sampled was somewhat less than 1% of the plateau. Similarly, the total time of sampling represents less than 4% of that encompassed by the austral spring/summer seasons. Hence, a legitimate question that can be asked is: how representative are the reported findings of plateau chemistry for the Austral spring/summer months? Clearly, the ANTCI airborne data set provides but a chemical snapshot of a small subregion of the plateau. Even given the large-scale meteorological analysis performed for the study period, the uniformity of different regions of the plateau, and the use of modeling products, optimistically no more than perhaps 20% of the plateau has been characterized. In spite of this limitation, the finding that there exists a reasonably high consistency between these observations and those recorded earlier at SP, it can be stated with relatively high confidence that the near-surface atmosphere over the plateau areas sampled is more like SP than unlike it. A notable exception to this conclusion involves the flight segments over fringe areas of the plateau (flights 10 and 12), which may have been influenced by inflow of marine air or other factors.

[50] Given these caveats, the findings from this study strongly suggest that the older chemical view of the plateau environment as simply providing a chemical graveyard for trace atmospheric constituents is in need of updating. The new chemical paradigm should not reject the graveyard characteristic, but rather add a major new component to it. This new dimension relates to the chemistry that occurs during the austral spring/summer time period. During this period the Antarctic plateau's shallow atmospheric BL routinely contains highly elevated concentrations of nitrogen oxides. As a result, large enhancements in the levels of reactive oxidizing species such as OH are also present. In simple chemical terms it means that this redefined atmosphere has the potential to chemically modify species before their deposition to the snow's surface, DMS being one such example. The available chemical evidence even suggests that this accelerated chemical activity extends below the uppermost layers of snow, in some cases modifying species even after their burial. The photodenitrification process involving the nitrate ion represents but one example of this.

[51] However, even with the above-cited advanced view of plateau chemistry, there still remain major unresolved issues. Among the most urgent is the uncertainty that persists regarding the plateau's surface NO<sub>x</sub> emission flux. Unlike other polar sites, the plateau displays extraordinarily high peak values of NO, in some cases reaching >1 ppbv. Equally significant, the time frame over which sudden concentration shifts can occur is frequently as short as 0.5 days. Our current understanding of polar meteorology and

photochemistry in a great many cases is unable to explain quantitatively these excessively high levels and the short time periods for the transition. Complicating this issue further is the uncertainty associated with our understanding of plateau HO<sub>x</sub>-NO<sub>x</sub> chemistry. For example, under plateau conditions the most recently developed polar chemical models predict that this highly nonlinear chemical system should lead to steady increases in the atmospheric lifetime of NO<sub>x</sub> with increasing NO<sub>x</sub> concentrations. In this scenario a given parcel of air can accommodate ever-increasing levels of NO<sub>x</sub>. Reflecting these modeling uncertainties, significant discrepancies still surface when comparing observations of HO<sub>x</sub> radical levels with those predicted. This suggests that current model mechanisms may not be representative of all major sources and sinks of one of the most critical species in the plateau's atmosphere.

[52] On a larger scale, there remains the very important and longstanding mystery regarding the sources of primary nitrogen to the plateau. Although this issue has been pursued for more than 30 years and numerous hypotheses have been put forth, no convincing answer has yet been found. As a result, we are still unable to use ice core nitrogen proxy data to make useful predictions regarding the oxidizing capacity of the planet's past atmosphere. Regarding this research team's efforts and those of many other investigators over the past 10 years, we still cannot say with great confidence how representative the latest chemical picture is of the larger plateau. Considering the small fraction of the plateau that has now been sampled, it indeed would be surprising if the vast unsampled regions produced no new scientific surprises. For example, we now know that fringe areas of the plateau can look very different from inland areas, but we still do not know if this is true for all fringe areas of the plateau. Some regions of the plateau also appear to be coupled to glacial valleys and thus potentially represent a significant source of NO<sub>x</sub> to coastal areas (unpublished results). So far, however, only 2 such areas out of 50 or more have been investigated. On a different front, it is thought by some researchers that the highest elevations on the plateau (~20% of the total surface area) could be the single largest source of NO<sub>x</sub> emissions. Currently, however, the only observations that address this issue are the limited ones near Vostok presented in this study. Finally, there continues to be considerable uncertainty regarding the extent to which shifts in latitude (sun angle effects) influence plateau surface emission rates and the resulting vertical distributions of NO<sub>x</sub>.

[53] Clearly, more detailed long-term chemical and meteorological plateau observations are needed. Although many of these might be carried out at SP, it will be critical that new sites such as Concordia [see, e.g., Legrand *et al.*, 2009], Vostok, Kohnen, Dome A, and Dome Fuji are examined. Additional aircraft studies will be needed to augment these fixed-site investigations. In particular, aircraft studies need to be designed to explore the large areas of the plateau that have no permanent measurement sites.

[54] **Acknowledgments.** Financial support for this research was provided by NSF Office of Polar Programs grants OPP-0229633 and OPP-0230246. We would also like to thank NOAA's Global Monitoring Division for their support of the ANTICI research effort at the South Pole ARO facility as well as Kenn Borek Air Ltd.'s ground and airborne staff for their dedication to making the Twin Otter sampling program a success.

## References

- Beine, H. J., F. Dominé, W. Simpson, R. E. Honrath, R. Sparapani, X. Zhou, and M. King (2002a), Snow-pile and chamber experiments during the Polar Sunrise Experiment "Alert 2000": Exploration of nitrogen chemistry, *Atmos. Environ.*, *36*(15–16), 2707–2719, doi:10.1016/S1352-2310(02)00120-6.
- Beine, H. J., R. E. Honrath, F. Dominé, W. R. Simpson, and J. D. Fuentes (2002b), NO<sub>x</sub> during background and ozone depletion periods at Alert: Fluxes above the snow surface, *J. Geophys. Res.*, *107*(D21), 4584, doi:10.1029/2002JD002082.
- Black, T. L. (1994), The new NMC mesoscale ETA-model—Description and forecast examples, *Weather Forecast.*, *9*(2), 265–278, doi:10.1175/1520-0434(1994)009<0265:TNNMEM>2.0.CO;2.
- Bromwich, D. H., J. J. Cassano, T. Klein, G. Heinemann, K. M. Hines, K. Steffen, and J. E. Box (2001), Mesoscale modeling of katabatic winds over Greenland with the Polar MMS, *Mon. Weather Rev.*, *129*(9), 2290–2309, doi:10.1175/1520-0493(2001)129<2290:MMOKWO>2.0.CO;2.
- Cassano, J. J., T. R. Parish, and J. C. King (2001), Evaluation of turbulent surface flux parameterizations for the stable surface layer over Halley, Antarctica, *Mon. Weather Rev.*, *129*(1), 26–46, doi:10.1175/1520-0493(2001)129<0026:EOTSFP>2.0.CO;2.
- Chen, G., et al. (2001), An investigation of South Pole HO<sub>x</sub> chemistry: Comparison of model results with ISCAT observations, *Geophys. Res. Lett.*, *28*(19), 3633–3636, doi:10.1029/2001GL013158.
- Chen, G., et al. (2004), A reassessment of HO<sub>x</sub> South Pole chemistry based on observations recorded during ISCAT 2000, *Atmos. Environ.*, *38*(32), 5451–5461, doi:10.1016/j.atmosenv.2003.07.018.
- Crawford, J. H., et al. (2001), Evidence for photochemical production of ozone at the South Pole surface, *Geophys. Res. Lett.*, *28*(19), 3641–3644, doi:10.1029/2001GL013055.
- Davis, D., et al. (2001), Unexpected high levels of NO observed at South Pole, *Geophys. Res. Lett.*, *28*(19), 3625–3628, doi:10.1029/2000GL012584.
- Davis, D., et al. (2004), South Pole NO<sub>x</sub> chemistry: An assessment of factors controlling variability and absolute levels, *Atmos. Environ.*, *38*(32), 5375–5388, doi:10.1016/j.atmosenv.2004.04.039.
- Davis, D. D., et al. (2008), A reassessment of Antarctic plateau reactive nitrogen based on ANTICI 2003 airborne and ground based measurements, *Atmos. Environ.*, *42*(12), 2831–2848, doi:10.1016/j.atmosenv.2007.07.039.
- Domine, F., and P. B. Shepson (2002), Air-snow interactions and atmospheric chemistry, *Science*, *297*(5586), 1506–1510, doi:10.1126/science.1074610.
- Eisele, F., et al. (2008), Antarctic tropospheric chemistry investigation (ANTICI) 2003 overview, *Atmos. Environ.*, *42*(12), 2749–2761, doi:10.1016/j.atmosenv.2007.04.013.
- Finlayson-Pitts, B. J., and J. N. Pitts Jr. (2000), *The Chemistry of the Upper and Lower Atmosphere: Theory, Experiments, and Applications*, Academic, San Diego, Calif.
- Gierczak, T., E. Jiménez, V. Riffault, J. B. Burkholder, and A. R. Ravishankara (2005), Thermal decomposition of HO<sub>2</sub>NO<sub>2</sub> (peroxynitric acid, PNA): Rate coefficient and determination of the enthalpy of formation, *J. Phys. Chem. A*, *109*(4), 586–596, doi:10.1021/jp046632f.
- Grannas, A. M., et al. (2007), An overview of snow photochemistry: Evidence, mechanisms and impacts, *Atmos. Chem. Phys.*, *7*(16), 4329–4373.
- Helmig, D., B. Johnson, S. J. Oltmans, W. Neff, F. Eisele, and D. D. Davis (2008a), Elevated ozone in the boundary layer at South Pole, *Atmos. Environ.*, *42*(12), 2788–2803, doi:10.1016/j.atmosenv.2006.12.032.
- Helmig, D., B. J. Johnson, M. Warshawsky, T. Morse, W. D. Nedd, F. Eisele, and D. D. Davis (2008b), Nitric oxide in the boundary-layer at South Pole during the Antarctic Tropospheric Chemistry Investigation (ANTICI), *Atmos. Environ.*, *42*(12), 2817–2830, doi:10.1016/j.atmosenv.2007.03.061.
- Honrath, R. E., M. C. Petersen, S. Guo, J. E. Dibb, P. B. Shepson, and B. Campbell (1999), Evidence of NO<sub>x</sub> production within or upon ice particles in the Greenland snowpack, *Geophys. Res. Lett.*, *26*(6), 695–698, doi:10.1029/1999GL900077.
- Honrath, R. E., S. Guo, M. C. Peterson, M. P. Dziobak, J. E. Dibb, and M. A. Arsenault (2000a), Photochemical production of gas phase NO<sub>x</sub> from ice crystal NO<sub>3</sub>, *J. Geophys. Res.*, *105*(D19), 24,183–24,190, doi:10.1029/2000JD900361.
- Honrath, R. E., M. C. Peterson, M. P. Dziobak, J. E. Dibb, M. A. Arsenault, and S. A. Green (2000b), Release of NO<sub>x</sub> from sunlight-irradiated mid-latitude snow, *Geophys. Res. Lett.*, *27*(15), 2237–2240, doi:10.1029/1999GL011286.
- Huey, L. G., et al. (2004), CIMS measurements of HNO<sub>3</sub> and SO<sub>2</sub> at the South Pole during ISCAT 2000, *Atmos. Environ.*, *38*(32), 5411–5421, doi:10.1016/j.atmosenv.2004.04.037.

- Jiménez, E., T. Gierczak, H. Stark, J. B. Burkholder, and A. R. Ravishankara (2004), Reaction of OH with HO<sub>2</sub>NO<sub>2</sub> (peroxynitric acid): Rate coefficients between 218 and 335 K and product yields at 298 K, *J. Phys. Chem. A*, *108*(7), 1139–1149, doi:10.1021/jp0363489.
- Jiménez, E., T. Gierczak, H. Stark, J. B. Burkholder, and A. R. Ravishankara (2005), Quantum yields of OH, HO<sub>2</sub> and NO<sub>3</sub> in the UV photolysis of HO<sub>2</sub>NO<sub>2</sub>, *Phys. Chem. Chem. Phys.*, *7*(2), 342–348, doi:10.1039/b413429j.
- Johnson, B. J., D. Helmig, and S. J. Oltmans (2008), Evaluation of ozone measurements from a tethered balloon-sampling platform at South Pole Station in December 2003, *Atmos. Environ.*, *42*(12), 2780–2787, doi:10.1016/j.atmosenv.2007.03.043.
- Jones, A. E., R. Weller, E. W. Wolff, and H.-W. Jacobi (2000), Speciation and rate of photochemical NO and NO<sub>2</sub> production in Antarctic snow, *Geophys. Res. Lett.*, *27*(3), 345–348, doi:10.1029/1999GL010885.
- Kalnay, E., et al. (1996), The NCEP/NCAR 40-year reanalysis project, *Bull. Am. Meteorol. Soc.*, *77*(3), 437–471, doi:10.1175/1520-0477(1996)077<0437:TNYRP>2.0.CO;2.
- King, J. C., S. A. Argentini, and P. S. Anderson (2006), Contrasts between the summertime surface energy balance and boundary layer structure at Dome C and Halley stations, Antarctica, *J. Geophys. Res.*, *111*, D02105, doi:10.1029/2005JD006130.
- Lefér, B. L., S. R. Hall, L. Cinquini, and R. E. Shetter (2001), Photolysis frequency measurements at the South Pole during ISCAT-98, *Geophys. Res. Lett.*, *28*(19), 3637–3640, doi:10.1029/2000GL012562.
- Legrand, M., and R. J. Delmas (1987), A 220-year continuous record of volcanic H<sub>2</sub>SO<sub>4</sub> in the Antarctic ice-sheet, *Nature*, *327*(6124), 671–676, doi:10.1038/327671a0.
- Legrand, M., and C. Feniet-Saigne (1991), Methanesulfonic-acid in south polar snow layers—A record of strong El Niño, *Geophys. Res. Lett.*, *18*(2), 187–190, doi:10.1029/90GL02784.
- Legrand, M. R., and S. Kirchner (1990), Origins and variations of nitrate in South Polar precipitation, *J. Geophys. Res.*, *95*(D4), 3493–3507, doi:10.1029/JD095iD04p03493.
- Legrand, M., and P. Mayewski (1997), Glaciochemistry of polar ice cores: A review, *Rev. Geophys.*, *35*(3), 219–243, doi:10.1029/96RG03527.
- Legrand, M., S. Preunkert, B. Jourdain, H. Gallée, F. Goutail, R. Weller, and J. Savarino (2009), Year-round record of surface ozone at coastal (Dumont d'Urville) and inland (Concordia) sites in East Antarctica, *J. Geophys. Res.*, *114*, D20306, doi:10.1029/2008JD011667.
- Mauldin, R. L., et al. (2001), Measurements of OH, H<sub>2</sub>SO<sub>4</sub>, and MSA at the South Pole during ISCAT, *Geophys. Res. Lett.*, *28*(19), 3629–3632, doi:10.1029/2000GL012711.
- Mauldin, R. L., III, et al. (2004), Measurements of OH, HO<sub>2</sub>+RO<sub>2</sub>, H<sub>2</sub>SO<sub>4</sub>, and MSA at the South Pole during ISCAT 2000, *Atmos. Environ.*, *38*(32), 5423–5437, doi:10.1016/j.atmosenv.2004.06.031.
- Mauldin, R., et al. (2009), South Pole Antarctica observations and modeling results: New insights on HO<sub>x</sub> radical and sulfur chemistry, *Atmos. Environ.*, *44*(4), 572–581, doi:10.1016/j.atmosenv.2009.07.058.
- Neff, W. D. (1999), Decadal time scale trends and variability in the tropospheric circulation over the South Pole, *J. Geophys. Res.*, *104*(D22), 27,217–27,251, doi:10.1029/1999JD900483.
- Neff, W., et al. (2008), A study of boundary layer behavior associated with high NO concentrations at the South Pole using a minisodar, tethered balloons and sonic anemometer, *Atmos. Environ.*, *42*(12), 2762–2779, doi:10.1016/j.atmosenv.2007.01.033.
- Oltmans, S. J., B. J. Johnson, and D. Helmig (2008), Episodes of high surface-ozone amounts at South Pole during summer and their impact on the long-term surface-ozone variation, *Atmos. Environ.*, *42*(12), 2804–2816, doi:10.1016/j.atmosenv.2007.01.020.
- Oncley, S. P., M. Buhr, D. H. Lenschow, D. Davis, and S. R. Semmer (2004), Observations of summertime NO fluxes and boundary-layer height at the South Pole during ISCAT 2000 using scalar similarity, *Atmos. Environ.*, *38*(32), 5389–5398, doi:10.1016/j.atmosenv.2004.05.053.
- Oppenheimer, C., et al. (2010), Plume chemistry and atmospheric impact of emissions from Erebus volcano, Antarctica, *J. Geophys. Res.*, *115*, D04303, doi:10.1029/2009JD011910.
- Ridley, B. A., and F. E. Grahek (1990), A small, low flow, high-sensitivity reaction vessel for no chemiluminescence detectors, *J. Atmos. Oceanic Technol.*, *7*(2), 307–311, doi:10.1175/1520-0426(1990)007<0307:ASLFHS>2.0.CO;2.
- Ridley, B. A., and L. C. Howlett (1974), An instrument for nitric oxide measurements in the stratosphere, *Rev. Sci. Instrum.*, *45*(6), 742–746, doi:10.1063/1.1686726.
- Ridley, B. A., F. E. Grahek, and J. G. Walega (1992), A small, high-sensitivity, medium-response ozone detector suitable for measurements from light aircraft, *J. Atmos. Oceanic Technol.*, *9*(2), 142–148, doi:10.1175/1520-0426(1992)009<0142:ASHSMR>2.0.CO;2.
- Ridley, B., et al. (2000), Is the Arctic surface layer a source and sink of NO<sub>x</sub> in winter/spring?, *J. Atmos. Chem.*, *36*(1), 1–22, doi:10.1023/A:1006301029874.
- Shetter, R. E., and M. Müller (1999), Photolysis frequency measurements using actinic flux spectroradiometry during the PEM-Tropics mission: Instrumentation description and some results, *J. Geophys. Res.*, *104*(D5), 5647–5661, doi:10.1029/98JD01381.
- Sinclair, M. R. (1981), Record-high temperatures in the Antarctic—A synoptic case-study, *Mon. Weather Rev.*, *109*(10), 2234–2242, doi:10.1175/1520-0493(1981)109<2234:RHTITA>2.0.CO;2.
- Slusher, D. L., S. J. Pittner, B. J. Haman, D. J. Tanner, and L. G. Huey (2001), A chemical ionization technique for measurement of pernitric acid in the upper troposphere and the polar boundary layer, *Geophys. Res. Lett.*, *28*(20), 3875–3878, doi:10.1029/2001GL013443.
- Slusher, D. L., et al. (2002), Measurements of pernitric acid at the South Pole during ISCAT 2000, *Geophys. Res. Lett.*, *29*(21), 2011, doi:10.1029/2002GL015703.
- Swanson, A. L., D. D. Davis, R. Arimoto, P. Roberts, E. L. Atlas, F. Flocke, S. Meinardi, F. S. Rowland, and D. R. Blake (2004), Organic trace gases of oceanic origin observed at South Pole during ISCAT 2000, *Atmos. Environ.*, *38*(32), 5463–5472, doi:10.1016/j.atmosenv.2004.03.072.
- van As, D., M. R. van den Broeke, and M. M. Helsen (2006), Structure and dynamics of the summertime atmospheric boundary layer over the Antarctic Plateau: 1. Measurements and model validation, *J. Geophys. Res.*, *111*, D07102, doi:10.1029/2005JD005948.
- van As, D., M. R. van den Broeke, and M. M. Helsen (2007), Strong-wind events and their impact on the near-surface climate at Kohnen Station on the Antarctic Plateau, *Antarct. Sci.*, *19*(4), 507–519, doi:10.1017/S095410200700065X.
- Wang, Y., Y. Choi, T. Zeng, D. Davis, M. Buhr, L. G. Huey, and W. Neff (2008), Assessing the photochemical impact of snow NO<sub>x</sub> emissions over Antarctica during ANTICI 2003, *Atmos. Environ.*, *42*(12), 2849–2863, doi:10.1016/j.atmosenv.2007.07.062.
- Wolff, E. W., J. C. Moore, H. B. Clausen, C. U. Hammer, J. Kipfstuhl, and K. Fuhrer (1995), Long-term changes in the acid and salt concentrations of the Greenland ice core project ice core from electrical stratigraphy, *J. Geophys. Res.*, *100*(D8), 16,249–16,263, doi:10.1029/95JD01174.
- Wolff, E. W., A. E. Jones, S. J.-B. Bauguitte, and R. A. Salmon (2008), The interpretation of spikes and trends in concentration of nitrate in polar ice cores, based on evidence from snow and atmospheric measurements, *Atmos. Chem. Phys.*, *8*, 5627–5634.

A. Beyersdorf and D. R. Blake, School of Physical Sciences, University of California, Irvine, CA 92697, USA.

M. P. Buhr and H. W. Wallace, Air Quality Design, Golden, CO 80403, USA.

J. H. Crawford, NASA Langley Research Center, Hampton, VA 23681, USA.

D. D. Davis (corresponding author), L. G. Huey, S. Kim, D. J. Tanner, Y. Wang, and T. Zeng, School of Earth and Atmospheric Sciences, Georgia Institute of Technology, Atlanta, GA 30332, USA. (douglas.davis@cas.gatech.edu)

F. L. Eisele, E. Kosciuch, and R. L. Mauldin, National Center for Atmospheric Research, Boulder, CO 80305, USA.

B. L. Lefér, Department of Earth and Atmospheric Sciences, University of Houston, Houston, TX 77204, USA.

W. D. Neff, Earth System Research Laboratory, NOAA, 325 Broadway, Boulder, CO 80309, USA.

D. L. Slusher, Department of Chemistry and Physics, Coastal Carolina University, Conway, SC 29526, USA.